Response to all reviewers.

General informations:

Changes in the manuscript are highlighted with dark red. *Italic* written text is the citation of the reviewers. Blue written text is the response of the authors. Longer text passages additionally included in the manuscript are highlighted with red. The revised version of the manuscript will be uploaded.

Response to review – RC1

Review of anonymous Referee #3

Remark: „*The authors present a study of humidity effects on filter-based absorption measurements. These effects may be important with UAV-based (low-power filter-based) absorption measurements where flight durations are relatively short and so the drone may not spend a lot of time at a fixed altitude. These are some interesting experiments, and the authors nicely explain the theory of absorption measurements. I have not seen a lot of papers about the TAP, so this could have been a useful contribution. However, I have several concerns with this manuscript. It is not clear to me that the authors understand the instruments they use or what the data are telling them. Some key points are listed below:*"

Response:

We thank for the review. The reviewer focuses on UAV measurements. Though other applications for the STAP are available like in helicopter-borne and tethered balloon platforms. Ongoing we will address the key points of the reviewer point by point:

Key point 1: "*The TAP has a reference filter measurement, where the particle-free air downstream of the first filter is exposed to a reference measurement. This could explain why the TAP shows a lower response to humidity changes, and possibly why the sign of the effect is opposite that of the mini-Aeth. However, the authors fail to mention this crucial design difference.*"

Response:

Thanks for the comment. We totally agree that we forgot to mention that crucial difference in design. To determine the absorption coefficient, the MA200 also uses a reference spot through which no air flow is passing through. Therefore, *rh* changes have a larger impact for this instrument than for the STAP in which the reference spot downstream the sample spot is exposed to RH changes as well. We updated the sections 2.2.1 and 2.2.2 to provide a more detailed look into the design of the instruments. The sections are as follows:

"2.2.1 Single Channel Tri-color Absorption Photometer (STAP)

The Single Channel Tri-color Absorption Photometer. This photometer detects light intensities behind two quartz-fiber glass filter (PALL LifeScience, Pallflex Membrane Filters Type E70-2075W) at three wavelengths (450, 525 and 624 nm). On the first filter, the sample filter, the light attenuates due to

deposited particulate matter. The second filter, the reference filter, is located downstream the sample filter and allows blank filter reference light intensity measurements.

By default, the particle light absorption coefficient is determined internally using 60 s averages of the raw intensity measurements for both filter spots. Therefore, in Eq. (5) *I(t)* is defined as:

$$I(t) = \frac{I_{\mathrm{smp},\lambda}}{I_{\mathrm{ref},\lambda}}, \tag{7}$$

where I_{smp} and I_{ref} is the intensity of light at the certain wavelength λ behind the sample (smp) and blank reference (ref) filter, respectively. Nevertheless, all raw measurements are recorded with a time resolution of 1 Hz allowing a recalculation of σ_{abs} at this time resolution. The volumetric flow is set to one liter per minute (lpm). According to the manual, at an internal averaging interval of 60 s, the measurement uncertainty is specified to 0.2 Mm^{-1}. The spot diameter is ~4.8 mm which leads to a sample area of A_{spot} ~1.75e-5 m^2.

2.2.2 MA200

The second instrument used here is the microAeth® MA200 is a small sized (13.7 x 8.5 x 3.6 cm; 420g), absorption photometer measuring the attenuation of light at 5 wavelengths (375, 470, 528, 625, and 880 nm; 625 nm are investigated in this study) due to deposited particulate matter on a PTFE filter band.

Similarly to the STAP, the MA200 detects light intensities behind a sample and reference spot. The particulate matter samples on a sample spot with 3 mm diameter leading to a sample area of A_{spot} ~0.71e-5 m^2. The reference spot of same area allows for blank filter measurements. M_{eBC} is determined under the assumption that the change of attenuation is proportional to the deposited eBC mass. The measurements were recorded with a 1 Hz time resolution. With the DualSpot® technology the instrument is able to reduce uncertainties related to loading effects up to 60 % (Holder et al., 2018) but was not functioning at the time of the experiment.

Holder et al. (2018) reported that the measurements are slightly depending on *rh* and *T* of the aerosol sample. However, they observed concentrations of up to 7 mg m^{-3}, at which the observed dependence on humidity and temperature did not influence the measured values significantly. Furthermore, they used another version of the instrument (MA350), which may react differently to changes in humidity and temperature."

Key point 2: "*The effects due to humidity changes are *temporary*. This is shown by the rise in absorption followed by a return to normalcy. The authors try to explain the initial changes by speculations about physical phenomena, but the measurements return to that shown by normal, unaffected conditions even as the RH remains high. The water film or beads would not disappear if the humidity remains constant.*"

Response:

Thanks for that comment. We totally agree that the effects are temporary. But, the main focus of this paper is to highlight these temporary changes, since they are important, especially when a high temporal and spatial resolution is needed. The focus of our study is not on measurements with a long averaging time.

Indeed, the beads would not disappear. But after the filter equilibrates after humidity changes there is no change of the optical properties (attenuation) of the filter medium. Since only change of the attenuation of two subsequent measurements is important for the measured particle light coefficient a constant relative humidity has no effect on the measurements.

Key point 3: "*A lot of the manuscript focuses on 60-second average measurements. The typical flight time of a UAV is 30 minutes, maybe two hours maximum. At the short end, 60-second averages are not very useful. At the top end, the instrument has time to equilibrate at a particular altitude to wait out any RH effects.*"

Response:

Thanks for that comment. Indeed, for some applications the averaging period is too long. However, the 60-second averaging part of the paper, was intended to qualitatively describe the observed effect. The reaction of the instruments is also shown on a one second time base in Figure 3. These are important to resolve the effect of fast relative humidity changes which is necessary results to develop a correction scheme for the *rh* effect. Equilibration is not intended within this paper, since boundary layer physics, especially in the transition zone of mixing layer and free troposphere, do not allow for equilibration. Also measurements in clouds can be characterized by a fast changing relative humidity. Anyhow, we updated the manuscript by including Figure 3 to show the behavior of both instruments at 1 Hz time resolution in dependency of the *rh* change rate d*rh*/d*t*.

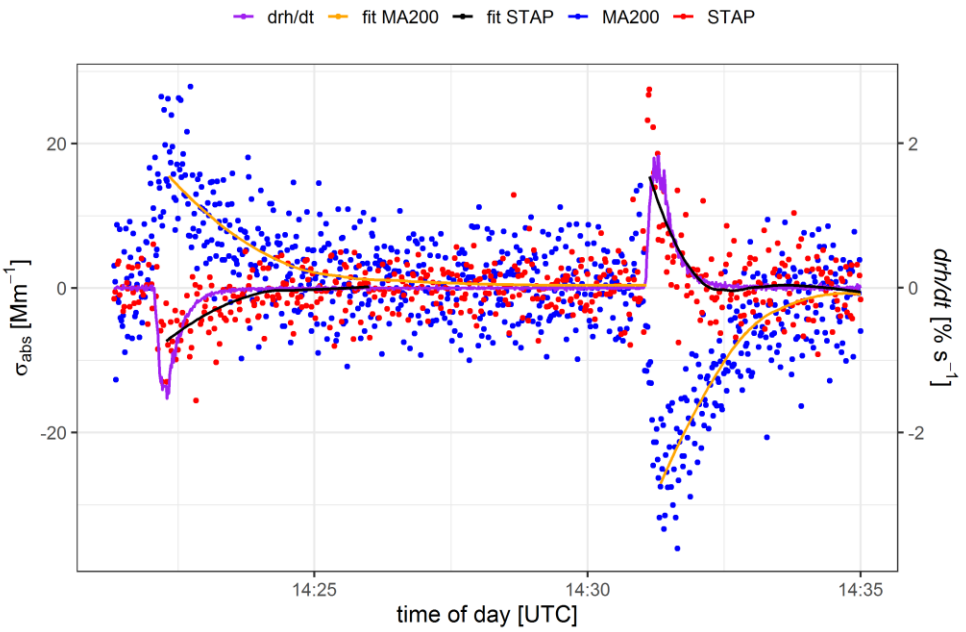

Figure 1: 1 Hz raw data of σ_{abs} at 625 nm measured by the MA200 (blue points) and recalculated at 624 nmSTAP200 (red points), the smooth fit through the measurements (orange and black), and d*rh*/d*t* (purple line).

Key point 4: "*The authors present an experiment showing that a dryer reduces the observed RH effects, but don't seem to understand or at least fail to explain why - the dryer likely reduces RH at the filter, so the effect on measured absorption should correspond to that at lower RH. This is seen by the similarity in slopes between the non-dryer and with-dryer cases. A key analysis would be (a) measuring the RH post-dryer; (b) comparing the effect at the post-dryer RH (say 90% pre-dryer, post-dryer 55%) to that at the same non-dryer RH (55%).*"

Response:

Thanks for that comment. We refer to anonymous referee #4 (RC2 supplement) that section 3.3 only describes that a dryer dries humidified air and recommends to omit this section. We therefore removed the section from the manuscript.

Key point 5: "*The authors compare the dry-to-wet and wet-to-dry changes without considering whether these changes are of the same magnitude both ways. There could be hysteresis effects, similar to particle hygroscopicity.*"

Response:

Thanks for that comment. We refer here to the scatter plot figures (Fig. 5 and 7 in the new manuscript) which clearly shows the dependency to the sign of the *rh* change. Obviously, the magnitudes are the same for both cases, at least on the basis of the used averaging period which might include a possible hysteresis effect. We clarified within the manuscript and added the sentence "As shown in Fig. 4, the magnitude of the deviation due to positive or negative changes in humidity is approximately the same for each device in terms of magnitude." at the end of Section 3.1. The sentence "Similar to the clean case, for both instruments, drying and humidifying the sample stream to the same extent resulted in a deviation of σ_{abs} with the similar magnitude." was added at the end of Section 3.2.1 and at the end of section 3.2.2 we added: "Overall, the magnitude of the deviation of σ_{abs} was independent of the sigh of humidity change for both instruments.".

Key point 6: "*The filter loadings and changes in RH considered here are ridiculously high. See for example doi:10.5194/amt-6-2115-2013; figure attached. RH changes are more gradual and Bap values are much, much lower, which suggests that we will not see the high spikes reported here (except maybe in biomass smoke plumes). The high filter loadings used here (~50 microg/m3) are likely exacerbating any effects.*"

Response:

Thanks for that comment. We agree, the filter loading concentrations are high. Anyhow, the loading periods where very short, and the attenuation due to loading with soot was never below 0.52 (extreme case), but the majority was above 0.74 which is a reasonable value for multi used filters or measurements in polluted conditions. Additionally, the filter loading concentrations cannot exacerbate the observed Considering *rh* change rates, we agree, especially in the case for 1 second average periods the change rates were pretty large. Anyhow, we also presented cases with change rates of -1.42 to 1.09 % s^{-1} which can be observed under real atmospheric conditions. Furthermore, since the observed points lying on the same line with a constant slope over all considered *rh* changes it is a satisfying assumption that the slope is also

valid for very small *rh* changes resulting in smaller bias. To point out that the filters were loaded before the humidified sample airstream was collected by the instruments we added: "Two main setups were used to investigate the effect of changes in real humidity. In the first, the filters of the devices were unloaded and the instruments collected a particle free airflow with adjustable relative humidity to examine the pure filter effect. In the second, the filters of the devices are loaded to a certain degree and afterwards they sample particle-free humidified air which accounts for the combination of both effects, the pure filter effect and the effect induced by the hygroscopic behavior of the particles." as second last paragraph in Section 2.3.

General point 1: "*There are other minor issues, and the manuscript needs an once-over by a native English speaker.*"

Response:

Thanks for that comment. We read over the manuscript and changed some unclear sentences. We refer here to the supplemented revised version of the manuscript in which all changes are documented.

Response to review – RC2

Review of anonymous Referee #4

Remark: „ *The paper describes the effects of variable humidity on measurements of light absorption with filter-based absorption photometers. It has been known for a long time that elevated relative humidity distorts these measurements and this is the main reason why it has been recommended to only use data sampled at dry conditions. In certain type of measurements, especially recently popular balloon or drone-borne vertical measurements drying is not possible and rh is rapidly changing. It is therefore important to characterize the responses of the absorption photometers to the changing conditions. This is what this paper presents. It is probably the first one that actually quantifies the effect.*

It is an interesting piece of work. For me the most interesting observation was the completely opposite response of the two absorption photometers and actually of the different filter materials. This very interesting indeed. Actually, it should be emphasized in the conclusions that the responses are filter material dependend and should be quantified if and when new filter materials are used in whatever filter-based absorption photometer, not just the two instruments used in this work. I can recommend the publication of the paper in AMT after some modifications. I did not find any major errors even though I did find some relatively small points to correct and change to the revised version of the ms. I will list them in the detailed comments below:"

Response:

We thank for the review. We will consider the general remark and emphasize, that it is a crucial task to quantify the effect of any absorption photometer, either by following our experimental setup or by other similar approaches. Especially since the STAP can operate with different filter material. Furthermore, more measurements regarding the MA200 have to be conducted to fully understand all the processes. In the conclusion is already stated that the opposing behavior is caused by the different filter material. As recommendation we added: "5. Since the response is different in magnitude and sign for both filter materials, we recommend to examine the effect for other filter materials as well."

The reviewer provided more comments and ongoing we will address them point by point:

Key point 1: "*L106. "Ogren (2010) published the loading correction ..." and then the Eq. (4) is shown. This is not quite correct. Ogren (2010) presented a corrected version of the equation which was originally presented and also corrected by Bond et al. (1999).*"

Response:

Thanks for that comment. We think the reviewer means that the sentence itself is wrong, and we update to: "For instance, Ogren (2010) reported an updated loading correction function for the PSAP introduced and updated by Bond et al. (1999) defined as:". We directly took the Eq. from the manual of the STAP so the Eq. (4) should be mentioned, since it is used internally.

Key point 2: "*L124-126 "... we used the σ_{abs} directly provided by the STAP and derived with the mentioned MAC in the case for the MA200, which already accounts for multiple scattering and filter loading corrections." How does MA200 account for multiple scattering and filter loading? What function is valid for Teflon? For STAP they are probably assumed to be done with the multiplication by Eq. (4), right?*"

Response:

Thanks for that comment. Yes, for the STAP the correction function from Eq. (4) is used internally by the STAP itself to account for filter loading effects. In the manual of the MA200 there is no loading correction function given. Anyhow, Jimenez et al. (2007) empirically determined a loading correction function *K(ATN)* for the Teflon filter-based AE41 and AE42 (Magee Scientific Company). This equation corrects the measured black carbon mass concentration M_{BC} as follows: $M_{BC} = \frac{b_{ATN}}{\sigma_{ATN}} \times \frac{1}{K(ATN)}$,

in which b_{ATN} is the attenuation coefficient in m^{-1} and σ_{ATN} the attenuation efficiency of BC with a value of 16.6 $m^2\ g^{-1}$ at 880 nm. *K(ATN)* is defined as:

$$K(ATN) = a + b \times \exp\left(\frac{-ATN}{100}\right),$$

with *a* and *b* some linear regression coefficients. Jimenez at al. (2007) reported values for *a* and *b* of 0.13 and 0.88. Besides that correction function, which could be applied during post-processing, the MA200 features a DualSpot© loading correction approach. Another Aethalometer (AE33) also uses the dual spot approach. A comprehensive correction approach using light attenuation measurements of two sample spots is provided by Drinovec et al. (2015). But, since the DualSpot© mode was not working during the time of the experiment, this also cannot be applied to the given data set. Hence, we suspect that there was no loading correction applied internally to the measurements of the MA200. Furthermore, since we do not know, if the MA200 needs the same loading correction of the AE41 or AE42, we did not consider any loading correction and decided to use the data directly measured by the instrument. This, if so, should only influence the results by a view per cent. As shown in the given manuscript, the areal loading density as well as the loading material do not change the response of the MA200 to *rh* changes. Therefore, we think a loading correction is negligible.

References: Jorge Jimenez, Candis Claiborn, Timothy Larson, Timothy Gould, ThomasW. Kirchstetter & Lara Gundel (2007) Loading Effect Correction for Real-Time AethalometerMeasurements of Fresh Diesel

Soot, Journal of the Air & Waste Management Association, 57:7,868-873, DOI: 10.3155/1047-3289.57.7.868

Drinovec, L., Močnik, G., Zotter, P., Prévôt, A. S. H., Ruckstuhl, C., Coz, E., Rupakheti, M., Sciare, J., Müller, T., Wiedensohler, A., and Hansen, A. D. A.: The "dual-spot" Aethalometer: an improved measurement of aerosol black carbon with real-time loading compensation, Atmos. Meas. Tech., 8, 1965-1979, https://doi.org/10.5194/amt-8-1965-2015, 2015.

Key point 3: "*2) The manufacturers, their addresses, and filter materials used in the photometers are presented on lines 79-82, lines 129-132, lines 135-137, and 147-150. Maybe once would be enough.*"

Response:

Thanks for that comment. Yes, we totally agree, that mentioning once is enough. Therefore, we removed the first, second and fourth mentioning and kept the manufactures addresses in the instrument description part. The used filter materials are important, therefore we think it is worth to repeat the used filter material several times to emphasize that.

Key point 4: "*L140. The reference to Holder et al. (2018) is to a conference abstract. I checked it at the conference book of abstracts. Sure, the abstract is there but it is so short that it does not contain any of the information you write on lines 139-145. If you cannot find anything that can be checked by a reader, you should remove these lines.*"

Response:

Thanks for that comment. The given reference refers to a poster presented during the 10th IAC in St. Louis, MO, USA. We updated the reference. We included the url which links to the webpage where the poster can be downloaded. This contains all the given information mentioned in the manuscript.

Holder, A., B. Seay, A. Brashear, T. Yelverton, J. Blair, and S. Blair. Evaluation of a multi-wavelength black carbon sensor, Poster, 10th International Aerosol Conference, St. Louis, MO, September 02 - 07, url: https://cfpub.epa.gov/si/si_public_record_report.cfm?Lab=NRMRL&dirEntryId=342614, 2018.

Key point 5: *"L213-214 "... Filter loading mass is calculated by multiplying the apparent loading mass concentration of the considered material..." What is apparent loading mass? Define it. Where do you get it from?"*

Response:

Thanks for that comment. We think we did not used the correct words to explain what we meant. We therefor reworded the 5th sentence in Section 3.2.: "For both considered loading materials, the mass loaded onto the filters was calculated by multiplying the prevalent loading mass concentration within the mixing chamber with the volume flow rate of the instrument and the loading duration.". The calculation of the prevalent loading mass concentration within the chamber is explained for both loading materials in the beginning of the Section 3.2.1 and 3.2.2 separately. For ammonium sulfate the ammonium sulfate

volume concentration (integral of the volume size distribution) within the chamber was multiplied an assumed ammonium sulfate density of 1.77 g/cm^{-3}. For BC different approaches had to be considered. We added: "During experiment #1 the mean absorption coefficient of the STAP was divided by a *MAC* of 6.6 m^2 g^{-1} since the absorption was stable during the loading period and it's a direct measure from the sampling instrument. For the experiment #2 the loading mass concentration was taken from the average of two consecutive MAAP measurements since the loading period was shorter than 2 minutes which is shorter than the internal averaging period of the STAP so that no stable absorption coefficient readouts could be provided by the STAP. During experiment #3 no MAAP was available and the absorption coefficient measured by the STAP was unstable. We therefore decided to estimate the loaded eBC mass by integrating the absorption coefficient during the loading period and dividing it by the *MAC*.". This should clarify how the loadings on the filters were derived. Furthermore, we think that the word "apparent" is wrong it that context.

Key point 6: "*L221-222 " Four different ρ* were .. for STAP, three for the MA200 ...". Were they not sampling simultaneously?*"

Response:

Thanks for that comment. For both instruments the first three filter areal loading densities were estimated simultaneously. Because of the lower flow rate and the different spot sizes these densities are different. The fourth loading density in the case of the BC was only estimated for the STAP since no MA200 was available during this time. Anyhow, the loading density is in the same range of previous loading periods and therefore at least on case with that areal loading density is covered. The MA200 was also not available during another ammonium sulfate experiment and therefore we have considered 11 areal loading densities for the STAP and 8 for the MA200 in this case. We changed the third last sentence in Section 2.3 to: "The loading aerosol was split into two streams from one of which the absorption photometer were sampling simultaneously." to emphasize that both photometer were sampling the same aerosol.

Key point 7: "*When I look at fig 5 I see that the time when ammonium sulfate was sampled was hours. How stable could you keep the AS production? How would possible instabilities affect the result?*"

Response:

Thanks for that comment. We consider, that we missed to explicitly point out that in the experiments considering different areal loading densities, the filter was loaded before the *rh* was changed. We therefore added the sentence:" The filter were loaded to a certain extent with different materials and afterwards the absorption photometer were sampling particle free air with adjustable humidity." In Section 3.2. Also we added:" Two main setups were used to investigate the effect of changes in real humidity. In the first the filters of the devices were unloaded and the instruments collected a particle free airflow with adjustable relative humidity. In the second, the filters of the devices are loaded to a certain degree and afterwards they sample particle-free humidified air." as the second last paragraph in Section 2.3.

The loading periods lasted 20 minutes at most. During the loading periods we generated ammonium sulfate with an atomizer, which produces very stable loading mass concentrations (narrow standard

deviation around the mean particle number and volume size distribution in Figure 2) when the aerosol chamber is well-mixed. Only during the well-mixed states of the mixing-chamber the filters were loaded. We added: "The very narrow standard deviation around the mean particle number and volume size distribution in Figure 2 indicate clearly that the loading mass concentrations were very stable during the loading periods." at the end of the first paragraph in Section 3.2.2.

Key point 8: "*L257-261. There is speculation about possible effects of the negligibly small imaginary index of AS. There is a more plausible explanation. Why wouldn't the explanation be the apparent absorption or cross sensitivity of any filter-based absorption photometer to purely scattering aerosol that the authors are well aware of? The apparent absorption should be mentioned and discussed at some point of the paper already earlier.*"

Response:

Thanks for that comment. This part is speculative and we removed the very negligibly small imaginary part of ammonium sulfate as a possible explanation. We agree that the cross-sensitivity of the absorption photometer to purely scattering aerosol is more important. The problem is, that the sensitivity to ammonium sulfate (Fig 6., measuring absorption during the loading period around 18:30 and 21:00 UTC) is also visible for the MA200 and it is not showing any variation in the response to relative humidity changes across different loading materials which could mean that PTFE membrane filter is unaffected by filter loading in terms of the *rh* effect or the loading was too low. This has to be tested in further studys. Anyhow, we updated the 5th paragraph in Section 3.2.2 to: "As shown in Fig. 6, both absorption photometers measure an "apparent" absorption coefficient of approximately 2 Mm^{-1} during loading with ammonium sulfate (18:30 and 21:00 UTC). This shows that absorption photometers react sensitively to scattering aerosols such as ammonium sulfate. The scattering ability of any material can be described with the real part of its refractive index. It seems that for the STAP the slope of the correlation increases with increasing scattering of the loading material (0.15 Mm^{-1} $\%^{-1}$ for a clean filter, 0.21 Mm^{-1} $\%^{-1}$ for ammonium sulfate, and 0.30 Mm^{-1} $\%^{-1}$ for BC). Ammonium sulfate has a real part of 1.521 ± 0.002 (at 532 nm Dinar et al, 2007) and BC from combustion processes has a real part of 1.96 at 530 nm (Kim et al., 2015 following Ackermann and Toon (1981)). Hence, the quartz fiber glass filters loaded with "artificially" absorbing aerosol inside the STAP could lead to a variation in the response to relative humidity changes. But, the MA200 was loaded with ammonium sulfate as well and its response to relative humidity changes is almost constant for all considered loading materials. Therefore, either the observation is caused by the interaction of quartz fiber glass filters with the loading material and the PTFE filter inside the MA200 do not causes this behavior, the filter loading of the MA200 was too low, or there are other mechanisms explaining this. Furthermore, since only three different cases (clean, ammonium sulfate and BC) were observed in this study more materials should be considered to investigate this phenomenon.".

Key point 9: "*Section 3.3. This section contains no other information but that a dryer dries humid air. The points in fig 7 are on the same line with and without drying so it does not tell anything about the responses of the absorption photometers. You would have obtained the same points also by reducing the original humidity. Even hypothetically there should not be a difference in reducing the original humidity or reducing it afterwards with a drier. Just omit the section.*"

Response:

Thanks for that comment. You are right. We omitted the Section since no new findings are given.

Key point 10: "*L325-326. Please show a scatter plot of the exponential decay, not only the time series.*"

Response:

Thanks for that comment. We are not quite sure what you mean with showing the exponential decay with a scatter plot in particular. Showing the decay for all investigated points is not helpful since the 1 Hz data is a) very noisy and b) the magnitude depends on the *rh* change and is c) biased due to the response time of the *rh* sensor. Therefore we added a new Figure (Figure 3) displaying the exponential decay exemplarily for *rh* change periods at 14:22 UTC and 14:32 UTC (*rh* change from Fig. 4 at the same time). We added:"

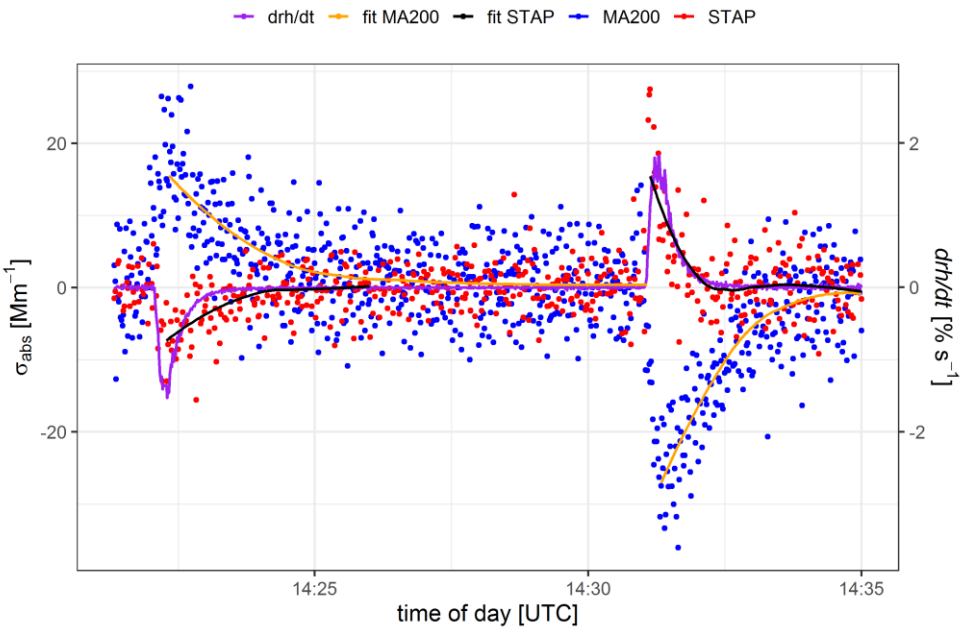

Figure 3: 1 Hz raw data of σ_{abs} at 625 nm measured by the MA200 (blue points) and STAP200 (red points), the smooth fit through the measurements (orange and black) and d*rh*/d*t* (purple line)."

and referenced to this Fig. within the text : "The exponential recovery behavior of the MA200 (see Figure 1) requires a more complex approach to correct for relative humidity changes." (first sentence ins Sect. 3.3.2) and also we mentioned the exponential recovery behavior in the beginning of Sect. 3: "This chapter will give an overview of the measurement results. The overall behavior of both instruments will be shown for wavelengths of 624 nm in the case of the STAP and 625 nm in the case of the MA200, respectively. A closer look at the behavior of both devices at 1 Hz time resolution shows that both devices differ greatly in quality (see Figure 3). The STAP (red dots and the smooth fit shown as black line) reacts very fast to

relative humidity changes (d*rh*/d*t* as purple line) and then returns relatively fast to the zero line. The MA200, on the other hand, also shows a fast response to relative humidity changes, but then shows a distinct exponential recovery (see Figure 3, blue dots and smooth fit shown as orange line) and reports absorption coefficients although there is no *rh* change.". The smooth fit (orange line) clearly indicates an exponential recovery behavior.

Key point 11: "*Explain clearly in the text and in the figure captions what is the difference between figs 3 and 5 and figs 4 and 6.*"

Response:

Thanks for that comment. Caption of Figure 4 is now: "Figure 4: Time series of *rh* (top panel) and absorption coefficient (bottom panel) measured with STAP (624 nm; black) and MA200 (625 nm; red) with clean filters." and of Figure 6: "Figure 6: *rh* of the air stream sampled by the MA200 and the STAP (upper panel) and σ_{abs} measured by MA200 and STAP at 625 (624) nm (lower panel). First up and down ramp of *rh* conducted with clean filter, second and third under conditions with filter loaded with ammonium sulfate. Loading periods around 18:30 and 21:00 UTC.". Caption of Figure 5 states now: " Figure 5: Scatter plot (dots) of all observations of the absolute excursion of σ_{abs} ($\Delta\sigma_{abs}$) in dependence of the absolute change in *rh* (Δrh), its linear regression fit as well as the summarizing boxplot of the linear regression fit are shown for the three investigated states (clean, loaded with BC and ammonium sulfate) at 624 nm (STAP, black colors) and 625 nm (MA200, red colors). Descriptive coefficients are given in Appendixtable 1." and correspondingly shows Fig. 7 the same plot but only considers the maximum and minimum areal loading density of the respective loading material. Caption of Fig. 7 states now: " Figure 7: Scatter plot of change in absorption ($\Delta\sigma_{abs}$) in dependence of the absolute change in *rh* (Δrh) separated into the different loading states (loaded with BC and ammonium sulfate) and minimum and maximum loading areal density on the filter. Dashed and colored lines represent the linear regression fit. Red and blue colors indicate MA200 at 625 nm and black and green colors indicate STAP at 624 nm. In the first panel BC loading is shown whereas in the second panel the ammonium sulfate case is displayed. Coefficients of the linear regression fit are displayed in panel 3. Shading of color in the linear fits and of the points are same as in panel 3."

The main difference between Fig. 4 and Fig. 6 is that in Fig. 6 smaller, stepwise *rh* changes were conducted. We updated the paragraph 3 in Section 3.2.2 to: "Figure 6 shows exemplarily the time series of *rh* of the sampled air *rh* and of the σ_{abs} measured with STAP and MA200 operated with clean filters. A *rh* of 0.0 to 96.2% with *drh/dt* humidity change rates of in the range of -1.42 and to 1.09 % s^{-1} was measured. Compared to the case in Figure 3 here a step-wise change of *rh* is shown. These steps resulted in a smaller absolute excursion of σ_{abs} which ranges from -7.2 to 9.0 Mm^{-1} (STAP; 624 nm, 60 s measurement resolution) and -14.1 to 10.9 Mm^{-1} (MA200; 625 nm, 60 second running mean). Furthermore, Figure 6 shows the response of the σ_{abs} to *rh* changes at three different states of filter loading. During the first ramp the filter were clean, during the second period the filters had a filter areal loading density of 32.5 (STAP) and 12.4 (MA200) mg m^{-2} and during the third ramp the filter in the STAP had loading areal density of 98.7 mg m^{-2} and the MA200 filter was loaded with an areal loading density of 37.6 mg m^{-2}. The response of the instruments during these periods is shown in Appendixtable 1."

The difference between Figure 4 and Figure 6 is that Fig. 4 shows the overall (mean) behavior of both instruments in BC and Ammonium sulfate case whereas Fig. 6 shows the response behavior of both instruments in cases of minimum and maximum loading of BC and Ammonium sulfate. The first sentence

in paragraph 4 Section 3.2.2 already states now: “In Figure 4 (lower left panel), the overall (mean) response of both instruments to *rh* changes is shown in the case of loading with ammonium sulfate.” The second last sentence in the last paragraph of Section 3.2.2 already stated: ”In Figure 6 (middle panel), the spread of the slopes within the shown cases is exemplarily shown for the investigated minimum and maximum load of the filters.”.

Response to review – RC3

Review of anonymous Referee #1

Remark: „*Düesing et al. have provided a systematic and detailed characterization of the bias of two widely-used commercial absorption photometers which results from exposure to step RH changes. While they have not solved the problems of these photometers, they have nevertheless provided useful quantitative data and useful correction schemes. The manuscript should be published in ACP after addressing all of my comments below. The most important comments are that the data must be weighted by uncertainties before fitting, that the running mean the authors used has smoothed the data (and likely biased the fits), and that complete uncertainties must be provided for the authors' correction schemes.*"

Response:

We thank for the review. We will consider the general remark. Regarding the weighting of the fittings. The *rh* sensor uncertainty is constant in absolute value of 1.8% up to 90% *rh*. But the sensor includes also a response time which has to be considered as well. This is a very complex task and we cannot estimate the uncertainty induced by that. Therefore a weighting by uncertainties is not possible. The reviewer provided detailed comments and ongoing we will address them point by point:

Key point 1: "*Section 2.1 (Theory of instruments) should be expanded to include mathematical statements of how the authors view the transient RH effects. In particular, it should be spelled out that M_{eBC} is based on the difference between subsequent attenuation measurements. This differential attenuation measurement also raises the possibility of investigating and correcting RH effects by looking directly at attenuation data. The authors should either look into this possibility, or discuss why they did not.*"

Response:

Thanks for that comment. We did not consider the attenuation because for most of the users of this instruments the particle light absorption coefficient and the eBC mass concentration are more intuitive.

Considering the effect of water in form of water vapor expressed as relative humidity we changed after Eq. (5): " *Water has a refractive index of 1.33+i1.5e-9 at 532 nm wavelength. Hence it interacts with incoming electromagnetic radiation. If the filter is exposed to a relative humidity changes the light attenuation of the filter changes simultaneously, since the water binds to the filter itself (Caroll, 1976 and Caroll, 1986). Since a variety of filter materials, with different physical properties exist, we suspect that magnitude and sign of the light attenuation coefficient can vary with the filter material. The hypothesis is that the change rate of the rh (drh/dt) directly determines the magnitude of the particle light absorption coefficient, which depends on the difference of two subsequent attenuation measurements.*". We think that clarifies the paragraph.

Key point 2: "*The use of a running mean for the MA200 means that the results are not equivalent to the 1-minute mean of the STAP. The running mean approach needs to be reconsidered. First, a running 60-second mean results in smoothing since each data point is used 3 times. Therefore the linear fits and R2 values reported are invalid since R2 is artificially enhanced by the autocorrelation which is inherent in a running mean. Best practice would be to analyze the 1-sec MA200 data and 60-sec mean MA200 data. The difference will provide insight into the STAP's limited time resolution. This point is related to my next point.*"

and

Key point 3: "*The changes in Figure 3 are rapid relative to the 1-minute averaging intervals used. This means that the signal cannot be accurately represented by a single value (mean) during periods of change (increasing/decreasing RH). I would predict that increasing/decreasing RH periods have systematically different biases in the residuals of Figure 4. To correctly account for these biases, uncertainties must be estimated and an orthogonal regression must be performed in Figure 4, after weighting by these uncertainties. Most scientific software packages support this. Afterwards please highlight periods of increasing/decreasing RH in Figure 4 (eg with different symbols).*"

Response to point 2 and 3:

Thanks for that comments. We choose the given averaging periods to show the general behavior of both instruments. For correction, the 1 Hz data of instruments were used. The linear regression is not artificially enhanced since we selected discrete points in the time series for the correlation. We described the method in the beginning of Section 3: "*This chapter will give an overview of the measurement results. The overall behavior of both instruments will be shown for wavelengths of 624 nm in the case of the STAP and 625 nm in the case of the MA200, respectively. A closer look at the behavior of both devices at 1 Hz time resolution shows that both devices differ greatly in quality. The STAP reacts very fast to relative humidity changes (see Figure 3, red dots and orange line) and then returns relatively fast to the zero line. The MA200, on the other hand, also shows a fast response to relative humidity changes, but then shows a distinct exponential recovery (see Figure 3) and reports absorption coefficients different from zero although there is no rh change.*

Therefore, we use an averaging on a 60 second basis to describe the qualitative behavior of both devices. In the case of the STAP, the internal 60 second averaging is used. For the MA200, on the other hand, a 60-second "running average" is applied to the 1 Hz measurements.

The qualitative behavior of both devices is shown as follows. To each absolute change in the relative humidity (Δrh) the corresponding maximum of the excursion of the averaged absorption coefficient ($\Delta\sigma_{abs}$) has been assigned. Where the absolute change of the relative humidity is the difference between the relative humidity at the time of the largest excursion in the absorption coefficient and the relative humidity at the start of the excursion. This approach also excludes the response time of the rh sensor.

First, the results for the pure filter effect will be shown. Afterwards, we present the results of the combined behavior of filter and aerosol particles on the filters. For loaded filters, the combined effect will be shown separated into BC and ammonium sulfate loaded filter."

Furthermore, the STAP has no limited time resolution since it reports the raw intensities with a 1Hz resolution and from which the light absorption coefficient can be calculated based on Eq. (5). Anyhow, the different behavior of both instruments on a 1 Hz measurement resolution (exponential recovery of the MA200, see Fig. 3) led to the conclusion that we apply a running mean to the data of the MA200, which is

similar to the internal running average of the STAP to describe the qualitative behavior of both instruments on that time base. Also, we included, that the *rh* sensor has a response time (t_{63}) of less than 10 s (see sensor specifications) as the 2nd last sentence in paragraph 3 of Sect. 2.3:" *Furthermore, this sensor has a response time t_{63} of <10s.*". The correlation of discrete points of the time series also accounts for that response time.

The scatter plot in Fig. 4 (now Fig. 5) shows the absolute change of absorption in dependency of the absolute change of *rh*. Therefore, the last non-excursed value (before *rh* change) of the absorption coefficient was subtracted from the maximum value of the absorption coefficient during the excursion. This was assigned to the difference of the starting *rh* and the *rh* at the point of maximum excursion of σ_{abs}. To clarify we included the description of the method as shown above. We furthermore think, that it was unclear that we did not correlate the whole time series of *rh* and σ_{abs} but the difference of discrete points in the time series. We think the updates make this clearer. Therefore, the points in Fig. 4 (now Fig. 5) do not need another symbol since points estimated based on a positive *rh* change are located in the right half of the scatter plots.

Key point 4: "*The authors have speculated extensively about the cause of the opposite trends of quartz and PTFE (lines 197-200). This speculation is of little value without experimental support. But I am not requesting experimental support. I am rather suggesting that the authors use these insights to design an improvement — use a mixture of the MA200 and TAP approaches to cancel out some of the biases of each approach. The utility of this suggestion can be tested by "simulating" a new instrument using the authors' measurements. The design details related to feasibility of this should be commented on.*"

Response:

Thanks for that comment. Since the underlying processes, especially the exponential recovery behavior of the MA200, are not fully understood. A new instrument could contain two sampling spots with both filters to cancel out each other. For that the different magnitudes of the effects have to be considered as well. It is only speculative why the PTFE filter inside the MA200 shows a larger response to *rh* changes. Besides the flow not passing through the reference spot, also the lower flow rate could have an effect but was not investigated. Therefore, we think a "simulation" of a new instrument is not useful right now. Anyhow, we included a paragraph, which gives a first idea how such a new instrument could be designed: "Since the filter in the STAP reveals a positive and the filter in the MA200 a negative correlation to relative humidity changes a combination of both filters within one instrument could account for the observed effect. A new developed instrument could use these two different filter materials on two sampling spots to cancel out the effect of each other. Though, more investigations have to be done, especially to understand the different recovery behaviors and effect magnitudes of the PTFE and quartz-fiber filter.".

Key point 5: "*In Figure 7, why did the authors not simply sample for a longer time with the MA200 in order to match the loadings on either instrument?"*

Response:

Thanks for that comment. The loading of the STAP and MA200 under the given loading conditions can be converted to equivalent sampling periods of several hours depending on the prevalent ambient aerosol mass concentration. We wanted to keep these equivalent sampling equal for both instruments. Furthermore, under real life conditions the MA200 samples less particulate matter than the STAP by default due to the smaller flow rates.

Key point 6: "*Line 260, not only the imaginary part of refractive index but also the real part will affect these results, since the real part will influence scattering (influencing attenuation as well as subsequent absorption). Please reword.*"

Response:

Thanks for that comment. We overthought this and came to the conclusion that the imaginary part does not has an impact on the shown behavior since it is too small in the case of ammonium sulfate. We reworded also following the comments of anonymous referee #4 and we updated the 5th paragraph in Section 3.2.2 to: "As shown in Fig. 5, both absorption photometers measure an "apparent" absorption coefficient of approximately 2 Mm^{-1} during loading with ammonium sulfate (18:30 and 21:00 UTC). This shows that absorption photometers react sensitively to scattering aerosols such as ammonium sulfate. The scattering ability of any material can be described with the real part of its refractive index. It seems that for the STAP the slope of the correlation increases with increasing scattering of the loading material (0.15 Mm^{-1} $\%^{-1}$ for a clean filter, 0.21 Mm^{-1} $\%^{-1}$ for ammonium sulfate, and 0.30 Mm^{-1} $\%^{-1}$ for BC). Ammonium sulfate has a real part of 1.521 ± 0.002 (at 532 nm Dinar et al, 2007) and BC from combustion processes has a real part of 1.96 at 530 nm (Kim et al., 2015 following Ackermann and Toon (1981)). Hence, the quartz fiber glass filters loaded with "artificially" absorbing aerosol inside the STAP could lead to a variation in the response to relative humidity changes. But, the MA200 was loaded with ammonium sulfate as well and its response to relative humidity changes is almost constant for all considered loading materials. Therefore, either the observation is caused by the interaction of quartz fiber glass filters with the loading material and the PTFE filter inside the MA200 do not causes this behavior, the filter loading of the MA200 was too low, or there are other mechanisms explaining this. Furthermore, since only three different cases (clean, ammonium sulfate and BC) were observed in this study more materials should be considered to investigate this phenomenon."

Key point 8: "*The correction schemes are not perfect, but they are useful. Certainly these and other authors will apply them at some point. It is therefore very important to report UNCERTAINTIES for the correction schemes. Both a percentage uncertainty and a bias (absolute value, in analogy to limit of detection) uncertainty must be reported. The bias requirement is illustrated in Figure 10, where 2/Mm of false signal result from a step RH change of about 30%. This bias of 2/Mm means that a true signal of 1/Mm would hardly be measurable.*

I do not know of a formal reference for handling this kind of bias, but I have encountered it in my own work and thought a bit about an easily understandable solution. My best suggestion is to allow users to answer the question: what is the minimum reported value which I can trust, if I am willing to accept a maximum inaccuracy of 25%? This question can be answered with a simple mathematical formulation which I will leave for the authors to provide. The answer to this question (the actual bias) will obviously depend on the magnitude of Δrh."

Response:

Thanks for that comment. We reworded a major fraction of Section 3.3.1 including the correction scheme of the STAP. It states now:" In Figure 8 the correlation of *rh* change rate (d*rh*/d*t*) and the measured σ_{abs} at 624 nm measured by the STAP (red circles) and recalculated with respect to standard conditions (pressure of 1013.25 hPa and temperature 273.15 K) is shown. The STAP-based background eBC mass concentration during the experiment was ~190 ng m^3 (at standard conditions, σ_{abs} at 624 nm converted with a *MAC* of 6.6 m^2 g^{-1}), which corresponds to offset (standard conditions corrected values) in the shown scatterplot of Figure 8 and which has no influence on the response to *rh* changes as shown previously.

The *rh* change rate ranged from -10.8 to 14.5 % s^{-1}. These rates correspond to a σ_{abs} of -231 to 192 Mm^{-1} for recalculated values at standard conditions and -203 to 164 Mm^{-1} directly measured by the instrument. But these measurements are biased by the response time of the relative humidity sensor so that the "real" *rh* change-rate cannot fully represented by these measurements. On average the slope (correction factor C_{rh} in Eq. (8)) of the linear fit is 10.08 (± 0.12) Mm^{-1} s %$^{-1}$ for standard conditions and 8.82 (± 0.10) Mm^{-1} s %$^{-1}$ for direct instrument output, respectively. Calculating the particle light absorption coefficient introduced by *rh* changes with:

$$\sigma_{\mathrm{abs,rh}} = C_{\mathrm{rh}} \frac{\mathrm{d}rh}{\mathrm{d}t} \tag{8}$$

for different *rh* change rates in both, the recalculated and direct instrument output case, and subtracting it from measurements allows to correct for the observed effect as follows:

$$\sigma_{\mathrm{abs,corr}} = \sigma_{\mathrm{abs,meas}} - \sigma_{\mathrm{abs,rh}}\,, \tag{9}$$

and after replacing $\sigma_{abs,rh}$ in Eq. (8) with Eq. (9) follows:

$$\sigma_{\mathrm{abs,corr}} = \sigma_{\mathrm{abs,meas}} - C_{\mathrm{rh}} \frac{\mathrm{d}rh}{\mathrm{d}t}\,. \tag{10}$$

The y-intersect of the linear fit in Figure 8 has not to be considered for correction as mentioned before. Disadvantageously, with this correction the noise of the *rh* sensor will propagate in the corrected σ_{abs}.

Furthermore, the linear fit in Figure 8 under- or overestimates the behavior in regimes of very high relative humidity change rates most likely due to the response time of the *rh* sensor, so that the correction function cannot entirely correct the bias. Therefore, the given correction factor C_{rh} consists of uncertainties, which cannot be entirely addressed. Hence, it is only a first guess, needs further refinement and right now we do not recommend to use the correction approach as long the uncertainties are not fully addressed. Furthermore, since only one STAP was tested, other STAP may have other correction factors due to a unit to unit variability. Additionally, other filter materials used in the STAP can also lead to another behavior. Anyhow, the upper function was applied to STAP measurements conducted with the same *rh* sensor under atmospheric conditions.

Exemplarily, Figure 9 shows this application. The figure shows airborne measurements of σ_{abs} at 624 nm derived with the STAP derived during a campaign conducted in March 2017 in East Germany. The upper panel displays the *rh* of a dried aerosol sample stream measured upstream of the STAP. The lower panel shows the recalculated σ_{abs} at 624 nm wavelength corrected for *rh* changes (black) and biased by *rh* changes (red). In the periods where the *rh* changes relatively fast (d*rh*/d*t* of -0.55 to 0.56 % s^{-1} e.g. at around 6200 seconds), the uncorrected σ_{abs} overshoots. The correction significantly reduces this bias and smooth out the measurements during the periods of *rh* changes. At the peaks of d*rh*/d*t* the difference of the corrected and uncorrected values is up to 1.5 Mm^{-1}, which is significant with respect to the measured $\sigma_{abs.}$ The periods with negative σ_{abs} are not introduced by the *rh* effect. We moreover think that a small offset is introduced in the initialization process of the instrument. Despite the imperfection of the correction scheme, this linear approach can be useful to derive a rough estimate of the accuracy of the measurements. For instance let *x* be the required accuracy for the measurements in % and σ_{abs} the measured particle light absorption coefficient we can express the ambient particle light absorption coefficient which is at least needed to fulfill the accuracy criterion in dependency of the *rh* change rate d*rh*/d*t*:

$$\sigma_{\mathrm{abs,meas}} \geq \frac{100\%}{x[\%]} C_{\mathrm{rh}} \left[\frac{Mm^{-1}s}{\%}\right] \left|\frac{drh}{dt}\right| \left[\frac{\%}{s}\right]. \tag{11}$$

Exemplarily, if a change rate of 0.1 % s^{-1} is measured and an accuracy of 25% is needed, at least a measured particle light absorption coefficient of around 4 Mm^{-1} is needed to fulfill the accuracy criterion.".

The main reason why we did not provide any uncertainties of the correction scheme besides the uncertainty of the slope is that we simply cannot quantify the uncertainty introduced by the response time of the *rh* sensor. Furthermore, each *rh* sensor will have different characteristics so that the correction scheme, if any, can only be applied using this sensor. We moreover suggest to use the findings to estimate the measurement uncertainties introduced by *rh* changes and to set a lower threshold of reliable measurements depending on the required accuracy and prevalent *rh* change rate.

For the MA200, the problem is even more complex since the correction approach results in slightly different coefficients of the correction formula when applied to other similar experiments. This could be due to a unit-to-unit variability or other phenomena affecting the PTFE response so that not all uncertainties can be addressed. Furthermore, the response time of the *rh* sensor introduces some uncertainty to the correction approach which cannot be quantified. Since, we do not recommend to use the correction scheme providing uncertainties is of little value. Similar to the STAP the correction approach looks a) promising and shows the right direction and b) could be used to roughly estimate the bias in the measurements due to *rh* changes. Also, the last sentence of the second last paragraph and the last

paragraph of Section 3.3.2 states now: *"Here, the response time of the sensor could account at least for a part of the imperfection of the correction approach and cannot be fully quantified, yet.*

Unfortunately, the application of the same correction approach to other similar experiments resulted in different correction function a and b. Applying the approach to two clean case experiments from section 3.1 resulted in optimized parameters of a = -0.92 and -1.03 and b = 0.974 and 0.971, respectively. Hence, it is just a first step trying to account for relative humidity changes and further research with more MA200 simultaneously has to be done to fully understand the underlying processes and to fully quantify the uncertainties of the correction scheme Nevertheless, the presented approach significantly reduces the amplitude of the bias in the shown data set (see Figure 10). But, up to now we cannot recommend to use the given parameters to correct for rh effects. At most it can be used to make a rough estimate of how measurements of the particle light absorption coefficient derived the MA200 could be biased by rh changes.".

Minor comments:

We thank the reviewer for all the minor points, we will comment on each separately point by point.

Point 1: "*1. I would suggest taking the natural logarithm of Equations 1 and 2, or at least 2, so that the important terms (exponents of e) are more easily visible. Also, please at line 99 add a sentence clarifying that reinterpreting l as an aerosol path length does not mean that σ represents the aerosol absorption coefficient but still the filter attenuation coefficient.*"

Response:

We expressed Eq. (1) and Eq. (2) following the reviewer. In principle the theory should explain how the particle light absorption coefficient is derived. We followed the recommendations of the reviewer and added the sentence: "But, a reinterpretation of the path length does not mean that the result is the particle light absorption coefficient, but still the light attenuation coefficient.". But, we used the term light attenuation coefficient instead of filter attenuation coefficient.

Point 2: *"Line 116, please change "provide" to "report" since the photometers only estimate eBC."*

Response:

We changed according the referees comment.

Point 3*: "Comparison" by who, are those unpublished results from the authors' lab?*

Response:

Yes, these are unpublished results from the authors' lab and the data can be requested if needed. We changed the last paragraph in Sect. 2.1 to: "*Lab-comparison of the eBC mass concentration between a MAAP (Multi Angle Absorption Photometer; Thermo Fisher Scientific, 27 Forge Parkway, 02038 Franklin, MA, USA; Petzold and Schönlinner, 2004) at 637 nm wavelength and MA200 at 625 nm and STAP at 624*

nm beforehand the experiment revealed a good agreement within 3% and within 6%, respectively. For the STAP a MAC of 6.6 m^2 g^{-1} was assumed. Since a MAC of 6.6 m^2 g^{-1} is used for the MAAP at 637 nm, in this study we used the σ_{abs} directly provided by the STAP and derived with the mentioned MAC in the case for the MA200, which already accounts for multiple scattering and filter loading corrections."

Point 4*: "Line 138 and 155, I suggest SI units of area".*

Response:

Thanks for the comment. We are not sure what the reviewer means with Si-units of area. To our opinion m^2 is already a SI-unit.

Point 5:" *Line 167, change "by passing" to "by passing it through" (this sentence required 3 reads to be understood)"*

Response:

We updated to: "One of the flows was humidified by passing through two glass tubes containing distilled water at room temperature with an inlet and outlet for compressed particle free air.".

Point 6: *"I have not seen the term "floating mean" used before and an internet search did not bring up any definitions. I would recommend "running mean" (more precise, since floating implies complete freedom whereas running implies autocorrelation)."*

Response:

We changed each occurrence of floating mean with running mean.

Point 7: *The Section "Recommendations" should be a numbered section or subsection, and no sections should come after Conclusions.*

and

Point 8: *In Recommendations and the Introduction, the authors suggest avoiding fast changes by ascending slowly. This is simply not possible in some scenarios (unmixed layers, clouds) and this should be noted.*

Response to point 7 and 8:

Thanks for the comments. We removed the heading of the recommendations section and changed to the paragraph with the recommendations to: "The findings summarized above lead to following recommendations how to use this type of instruments:

1. When used for vertical profiling, apparent sharp gradients in *rh* during the profile have to be taken into account.
    a. The ascending speed of the profiling platform should be reduced if possible, to decrease the temporal change of *rh*, but in some scenarios this is simply not possible and therefore,

b. when fast relative humidity changes cannot be avoided, such periods have to be removed from the data set, or at least to estimate the uncertainties of the measurements based on the presented correction functions. Therefore,

2. we recommend recording the *rh* of the sampled aerosol. This allows to determine *rh* change rates. This allows to roughly estimate the bias of *rh* changes on filter-based absorption measurements with these two instruments.
3. The usage of a dryer is highly recommended, because it reduces the amplitude of the excursion in the measurements during fast *rh* changes.
4. For both instruments we recommend to conduct more similar experiments to address the flaws of our study to refine the presented correction approaches.
5. Since the response is different in magnitude and sign for both filter materials, we recommend to examine the effect for other filter materials as well.".

Also, we added in the last paragraph of the Abstract: "*Due to our findings, we recommend to use an aerosol dryer upstream of absorption photometers to reduce the rh effect significantly. Furthermore, when absorption photometers are used in vertical measurements, the ascending or descending speed through layers of large rh gradients has to be low to minimize the observed rh effect. But this is simply not possible in some scenarios especially in unmixed layers or clouds. Additionally, recording the rh of the sample stream allows correcting for the bias during post processing of the data. This data correction leads to reasonable results, according the given example in this study.*".

Point 9: *"Table 1: I see no bold entries."* and point 10*: "Table 2: Instead of custom formatting, add a column "Filter Number" which increases by 1 when appropriate."*

Response:

Thanks for the comment. We updated the tables to:"

Table 1: Filter loading mass concentration (M_{eBC}) of the black carbon particles and filter areal loading density (deposited mass per spot area) ρ^*_i. M_{eBC} were determined by dividing the average σ_{abs} of the STAP with an assumed MAC of 6.6 m^2 g^{-1} or based on the MAAP measurements. Usage of same filter is indicated by its filter number. Bold written entries were used for the investigation of the *rh* effect.

filter number	M_{eBC} [µg m^{-3}]	$\rho^*_{eBC,i}$ [mg m^{-2}]	
		STAP	**MA200**
#1	**44.5 (STAP)**	**14.0**	**5.4**
	43.4 (STAP)	37.9	14.4
	27.6 (STAP)	**42.9**	**16.3**
#2	**52.6 (MAAP, 2 scans)**	**2.8**	**1.1**
#3	-	**13.7 (integral of STAP)**	no data

Table 2: Average volume and mass concentration ($V_{(NH4)2SO4}$, $M_{(NH4)2SO4}$) of the loading $(NH_4)_2SO_4$ aerosol derived from the used MPSS (number of used scans in brackets) and loading areal density $\rho^*_{(NH4)2SO4}$ of the filters are given. Usage of same filter is indicated by its filter number, which means that the filter loading mass was adding up during the experiments.

filter number	$V_{(NH4)2SO4}$ [µm^3 cm^{-3}] (# scans)	$M_{(NH4)2SO4}$ [µg m^{-3}]	$\rho^*_{(NH4)2SO4}$ [mg m^{-2}]	
			STAP	MA200
#1	15.4 (2)	27.2	3.1	1.2
	18.6 (1)	32.9	10.5	4.0
	20.6 (3)	36.4	31.3	11.9
#2	20.6 (4)	36.5	40.8	15.5
#3	33.1 (3)	58.6	32.5	12.4
	33.5 (5)	59.3	98.7	37.6
#4	20.3 (3)	36.0	21.1	8.0
	20.3 (3)	36.0	41.9	15.9
#5	23.9 (3)	42.4	28.9	no data
	28.4 (4)	50.2	69.8	no data
	29.8 (2)	52.8	99.6	no data

The changes within the manuscript are manifold and we refer here to the marked-up version below, which contains all the changes.

The new Figure 3 is included in the supplemental material with all the other figures.

The effect of rapid relative humidity changes on fast filter-based aerosol particle light absorption measurements: uncertainties and correction schemes

Sebastian Düsing[1], Birgit Wehner[1], Thomas Müller[1], Almond Stöcker[2], Alfred Wiedensohler[1]

[1]Leibniz Institute for Tropospheric Research (TROPOS), 04318 Leipzig, Germany
[2]Ludwig-Maximilians-University Munich, Department of Statistics, 80539 Munich, Germany

Correspondence to: Sebastian Düsing (duesing@tropos.de)

Abstract.

Measuring vertical profiles of the particle light absorption coefficient by using absorption photometers may face the challenge of fast changes in relative humidity. These absorption photometers determine the particle light absorption coefficient due to a change in light attenuation through a particle-loaded filter. The filter material, however, takes up or releases water with changing relative humidity (*rh* in %), influencing thus the light attenuation.

A sophisticated set of laboratory experiments was therefore conducted to investigate the effect of fast *rh* changes (d*rh*/dt) on the particle light absorption coefficient (σ_{abs} in Mm^{-1}) derived with two absorption photometers. The *rh* dependency was examined based on different filter types and filter loadings with respect to loading material and loading areal density. ~~Different filter material was used in the two examined instruments.~~ The Single Channel Tri-Color Absorption Photometer ~~(STAP; Brechtel Manufacturing Inc, 1789 Addison Way, Hayward, CA 94544, USA)~~ relies on quartz-fiber filter ~~(PALL LifeScience, Pallflex Membrane Filters Type E70-2075W)~~ and the microAeth® MA200 ~~(AethLabs, 1640 Valencia St, Suite 2C, San Francisco, CA 94110, USA)~~ is based on a Polytetrafluoroethylene (PTFE) filter band. Furthermore, three cases were investigated: clean filter, filter loaded with black carbon (BC) and filter loaded with ammonium sulfate. The filter loading areal densities (ρ^*) ranged from 3.1 to 99.6 mg m^{-2} in the case of the STAP and ammonium sulfate, 1.2 to 37.6 mg m^{-2} considering the MA200. Investigating BC loaded cases, ρ^*_{BC} was in the range of 2.9 to 43.0 and 1.1 to 16.3 mg m^{-2} for the STAP and MA200, respectively. In addition, the effect of a silica-bead based diffusion on the *rh* effect was investigated.

Both instruments revealed opposing responses to relative humidity changes (Δ*rh*) with different ~~amplitudes~~magnitudes. ~~Whereas the~~ The STAP shows a linear dependence to relative humidity changes~~.~~, ~~t~~The MA200 is characterized by a~~n~~ distinct exponential recovery after its filter was exposed to relative humidity changes. At a wavelength of 624 nm and for the default 60~~-~~second running average output, the STAP reveals an absolute change in σ_{abs} per absolute change of *rh* ($\Delta\sigma_{abs}/\Delta rh$) of 0.14 Mm^{-1} $\%^{-1}$ in the clean case, 0.29 Mm^{-1} $\%^{-1}$ in the case of BC loaded filters, and 0.21 Mm^{-1} $\%^{-1}$ considering filters loaded with ammonium sulfate. The 60-second running average of the particle light absorption coefficient at 625 nm measured with the MA200 revealed a response of around -0.4 Mm^{-1} $\%^{-1}$ for all three cases. Whereas the response

of the STAP varies over the different loading materials, in contrast the MA200 was quite stable. The ~~minimum and maximum~~ response was for the STAP in the range of 0.17 Mm^{-1} $\%^{-1}$ ~~and~~ to 0.24 Mm^{-1} $\%^{-1}$ considering ammonium sulfate loading and in the BC loaded case 0.17 Mm^{-1} $\%^{-1}$ ~~and~~ to 0.62 Mm^{-1} $\%^{-1}$, respectively. In the ammonium sulfate case, ~~T~~the minimum response shown by the MA200 was -0.42 Mm^{-1} $\%^{-1}$ and -0.36 Mm^{-1} $\%^{-1}$ at maximum ~~for ammonium sulfate and,~~ -0.42 Mm^{-1} $\%^{-1}$ and -0.37 Mm^{-1} $\%^{-1}$ in case of BC loading, respectively. Using the aerosol dryer upstream, the STAP did not change the behavior, but the amplitude of the observed effect was reduced by a factor of up to three.

A linear correction function for the STAP was developed here. It is provided by correlating 1 Hz resolved recalculated particle light absorption coefficients ~~at 1 Hz time resolution against the~~and *rh* change rates ~~change rate of *rh*~~. The linear response is estimated with 10.08 Mm^{-1} s^{-1} $\%^{-1}$. Though, the uncertainties of the given correction approach could not be estimated due to the The provided correction function ~~and can be used to correct for bias induced to *rh* changes at this time resolution.~~ A correction approach for the MA200 is also provided, however, the behavior of the MA200 is more complex. Further research and multi-instrument measurements have to be conducted to fully understand the underlying processes, since the correction approach resulted in different correction parameters across various experiments. However, the exponential recovery after the filter of the MA200 experienced a *rh* change could be reproduced. Though, the given correction approach has to be estimated with other *rh* sensors as well since each sensor has a different response time. And, for the given correction approaches the uncertainties could not be estimated mainly due to the response time of the *rh* sensor. Therefore, we do not recommend to use the given approaches. But, they showing in the right direction and besides the imperfections they are useful to at least estimate the measurement uncertainties due to relative humidity changes.

Due to our findings, we recommend to use an aerosol dryer upstream of absorption photometers to reduce the *rh* effect significantly. Furthermore, when absorption photometers are used in vertical measurements, the ascending or descending speed through layers of large *rh* gradients has to be low to minimize the observed *rh* effect. But this is simply not possible in some scenarios especially in unmixed layers or clouds. Additionally, recording the *rh* of the sample stream allows correcting for the bias during post processing of the data. This data correction leads to reasonable results, according the given example in this study.

1 Introduction

Black carbon (BC) and its light-absorbing properties has significant influence on the Earth's climate, and its contribution is associated with major uncertainties, in particular due to its vertical distribution (Zarzycki and Bond, 2010). In addition, it is suspected to affect human health (WHO, 2012). Absorption photometer are feasible instruments to measure the light absorbing properties of aerosol particles. These photometers measure the aerosol particle light absorption coefficient (σ_{abs}) by detecting the change of attenuation of light due to deposited aerosol particle mass on sample filter. They have been installed on airship platforms (Rosati et al., 2016), tethered balloon platforms (Ran et al., 2016; Ferrero et al., 2014, Ferrero et al., 2016) or unmanned aircraft systems (UAS; Markowitz et al., 2017, Telg et al., 2017, Bärfuss et al., 2018) to address the

vertical BC distribution. To investigate human exposure to health-harming BC-containing aerosol particles from combustion sources, they have been used for mobile measurements (Capeda et al., 2017 and references therein; Alas et al, 2018).

Subramanian et al. (2007), Vecchi et al. (2013) and Lack et al. (2008) have shown, that liquid-like brown carbon can significantly bias filter-based absorption measurements since this organic carbon wraps around filter fibers and alters their structural properties. Aerosol samples contain water vapor represented by its relative humidity (*rh*). Similarly to the liquid-like brown carbons, during the sampling process, water vapor can be adsorbed by the filter material or might be bound on the binding material within the filters. A variety of filter materials is used in absorption photometers and the water uptake is different across various materials. Hence, changes in the aerosol *rh* can affect the aerosol particle light absorption measurements differently. Nessler et al. (2006) has shown to which extent sudden changes in relative humidity (*rh*) can influence measurements of a Particle/Soot Absorption Photometer (PSAP; Radiance Research, Seattle, WA) and an Aethalometer for clean filter material and loaded with BC, whereas Cai et al. (2014) has shown the effect for the microAeth® AE51, however, they did not quantify it. However, hygroscopic aerosol particle species such as ammonium sulfate can take up water depending on the relative humidity. The *rh* effect for filters loaded with such aerosol species was never quantified. Furthermore, not all filter materials have been covered within these studies. Summarizing, both, filter material and loading material, may influence the light attenuation of the filter.

The *rh* effect might not be relevant for averaging periods longer than 5 minutes as usually done at stationary measurements on ground (e.g. to address human exposure to BC containing aerosol particles). However, to address vertical profiling of BC with fast *rh* changes, particle light absorption measurements require a high temporal resolution of about seconds.

Telg et al. (2017) presented a study using an unmanned aircraft system (UAS) for vertical profiling of aerosol physical properties including the aerosol particle light absorption coefficient measured by an absorption photometer. In their study, a significant decrease of σ_{abs} at around 1000 m altitude is visible. Considering the other simultaneously measured microphysical aerosol parameters, this decrease is not to be expected. In the WMO/GAW report 227 (2016), it is recommended to conduct aerosol sampling below 40% relative humidity to prevent measurements artefacts due to high relative humidity. Although the measurements of Telg et al. (2017) have been conducted following these recommendations, this is a published example for the bias in σ_{abs} measurements due to fast *rh* changes even for a *rh* below the 40% threshold.

In our study, the *rh* effect is investigated for the small-sized photometers STAP ~~(Single Channel Tri-Color Absorption Photometer; Brechtel Manufacturing Inc, 1789 Addison Way, Hayward, CA 94544, USA)~~, using a quartz-fiber glass filter, and MA200® ~~(AethLabs, 1640 Valencia St, Suite 2C, San Francisco, CA 94110, USA)~~, which relies on a Polytetrafluoroethylene (PTFE) filter. We show results of a set of laboratory experiments and address the effect of sudden changes in relative humidity for both absorption photometers. Herein, we consider three different scenarios: a) clean filters, different filter loading densities of b) hydrophobic BC, and c) hydrophilic ammonium sulfate ($(NH_4)_2SO_4$). In all of these cases we also investigated the impact of a silica-bead based diffusion drier to the *rh* effect.

Following scientific questions will be addressed: To which extent do STAP and MA200 are sensitive to *rh* changes, and does different loading with respect to material and areal density contribute to this effect? Can the observed effect be corrected, and which recommendations can be given for the usage of such absorption photometer? This is important because recent developments indicate that lightweight absorption measuring instruments will be used more frequently for airborne applications in the near future.

2 Experiment

2.1 Theory of absorption measurements

Filter-based absorption photometer measuring the decrease of intensity of light which passes through the filter-medium with a specific optical thickness. The decrease of intensity can be described quantitatively according the law of Beer-Lambert:

$$\ln(I) = \ln(I_0) + \sigma_{\mathrm{ATN}}(\lambda) l \,, \tag{1}$$

where I is the attenuated intensity of light with a wavelength λ with a raw intensity I_0, attenuated along a path l through a medium with an light attenuation coefficient σ_{ATN}. The path length l can also be interpreted as the length of a column of aerosol passing through the sample area of the filter spot A_i of the instrument (subscript i), whereas the particles are collected and accumulated in the filter. But, a reinterpretation of the path length does not mean that the result is the particle light absorption coefficient, but still the light attenuation coefficient. ~~Therefore, t~~The path length l can be calculated by the volume, which flows at a certain rate (volume flow rate; Q_i), for a time Δt through the sample area A_i. Based on Eq. (1), this results~~, and hence we can rewrite Eq. (1) as~~into:

$$\ln(I(t)) = \ln(I(t-\Delta t)) + \sigma_{\mathrm{ATN,i}}(\lambda)\frac{Q_i \Delta t}{A_i} \,. \tag{2}$$

~~———~~While aerosol particles deposit on the filter the incoming light gets additionally scattered by those particles. Hence the effective pathway of the light through the filter increases due to the multiple scattering. To account for this, ~~in~~ Eq. (~~1~~2) needs $f(\tau)$, ~~is the~~ a transmission (τ) dependent filter-loading correction factor, with:

$$\tau = \frac{I(\mathrm{t})}{I_0} \,, \tag{3}$$

where I_0 is the light intensity measured ~~of~~ for a white, clean filter. For instance, Ogren (2010) ~~published~~ reported an updated ~~the~~ loading correction function for the PSAP introduced and updated by Bond et al. (1999) defined as:

$$f(\tau) = (1.0796\tau + 0.71)^{-1} \,, \tag{4}$$

which is also used for the STAP.

Rearranging and applying the filter loading correction to the attenuation coefficient Eq. (2) will give the particle light absorption coefficient~~Eq. (2) gives~~:

$$\sigma_{\mathrm{abs,i}}(\lambda) = \ln\left(\frac{I(t)}{I(t-\Delta t)}\right)\frac{f(\tau)A}{Q_{\mathrm{i}}\Delta t} \quad (5)$$

Water has a refractive index of 1.33+i1.5e-9 at 532 nm wavelength. Hence it interacts with incoming electromagnetic radiation. If the filter is exposed to relative humidity changes the light attenuation of the filter changes, since the water binds to the filter itself (Caroll, 1976 and Caroll, 1986). ~~Depending on the filter material this change increases or decreases the attenuation coefficient.~~Since a variety of filter materials, with different physical properties exist, we suspect that magnitude and sign of the light attenuation coefficient can vary with the filter material. The hypothesis is that the change rate of the *rh* (d*rh*/d*t*) directly determines the ~~amplitude~~ magnitude of ~~change in~~ the particle light absorption coefficient, which ~~is directly proportional to~~depends on the difference of two subsequent attenuation measurements.~~the change of attenuation.~~

The effect of changes in the relative humidity on particle light absorption measurements contains of two parts. First, the interaction of the filter with the *rh* by its own. Second, hygroscopic particles change their optical properties by the water uptake and loss due to growing and shrinking. Hence, aerosol particles under varying relative conditions will also have an effect on the reported particle light absorption coefficient.

Some absorption photometer such as the STAP directly ~~provide~~ report measurements of the aerosol particle light absorption coefficient σ_{abs}, some, for instance the MA200, ~~provide~~ report measurements of the equivalent black carbon (eBC; Petzold et al. (2013)) mass concentration (M_{eBC}). eBC mass concentrations can be converted to σ_{abs} with:

$$\sigma_{\mathrm{abs}} = M_{\mathrm{eBC}} \cdot MAC\,, \quad (6)$$

in which *MAC* is the mass absorption cross section in $m^2\ g^{-1}$.

Lab-c~~C~~omparison of the eBC mass concentration between a MAAP (Multi Angle Absorption Photometer; Thermo Fisher Scientific, 27 Forge Parkway, 02038 Franklin, MA, USA; Petzold and Schönlinner, 2004) at 637 nm wavelength and MA200 at 625 nm and STAP at 624 nm beforehand the experiment revealed a good agreement within 3% and within 6%, respectively. For the STAP a *MAC* of 6.6 $m^2\ g^{-1}$ was assumed. Since a *MAC* of 6.6 $m^2\ g^{-1}$ is used for the MAAP at 637 nm, in this study we used the σ_{abs} directly provided by the STAP and derived with the mentioned *MAC* in the case for the MA200, which already accounts for multiple scattering and filter loading corrections.

2.2 Instrument description

As mentioned before, we investigated two filter-based absorption photometers, which are described in the upcoming sections. The Single Channel Tri-Color Absorption Photometer (STAP; Brechtel Manufacturing Inc, 1789 Addison Way, Hayward, CA 94544, USA) and the MA200 (AethLabs, 1640 Valencia St, Suite 2C, San Francisco, CA 94110, USA) use different filter materials. The STAP relies on a quartz-fiber glass filter, whereas the MA200 is based on a Polytetrafluoroethylene (PTFE) filter. Since ~~T~~their behavior under fast changes of the relative humidity is not described yet and ~~hence~~ we investigate both instruments in this study.

~~2.2.1 MA200~~

~~The microAeth® MA200 is a small sized (13.7 x 8.5 x 3.6 cm; 420g), absorption photometer measuring the attenuation of light at 5 wavelengths (375, 470, 528, 625, and 880 nm; 625 nm are investigated in this study) due to deposited particulate matter on a Polytetrafluoroethylene (PTFE) filter band. The particulate matter samples on a sample spot with 3 mm diameter leading to a sample area of A_{spot} ~0.71e-5 m^2. M_{eBC} is determined under the assumption that the change of attenuation is proportional to the deposited eBC mass. The measurements were recorded with a 1 Hz time resolution. With the DualSpot® technology the instrument is able to reduce uncertainties related to loading effects up to 60 % (Holder et al., 2018) but was not functioning at the time of the experiment.~~

~~Holder et al. (2018) reported that the measurements are slightly depending on *rh* and *T* of the aerosol sample. However, they observed concentrations of up to 7 mg m^{-3}, at which the observed dependence on humidity and temperature did not influence the measured values significantly. Furthermore, they used another version of the instrument (MA350), which may react differently to changes in humidity and temperature.~~

2.2.1 Single Channel Tri-color Absorption Photometer (STAP)

~~The second instrument used here is the~~The Single Channel Tri-color Absorption Photometer ~~(STAP, Brechtel Manufacturing Inc, 1789 Addison Way, Hayward, CA 94544, USA)~~. This photometer detects light intensities behind two quartz-fiber glass filter (PALL LifeScience, Pallflex Membrane Filters Type E70-2075W) at three wavelengths (450, 525 and 624 nm). On the first filter, the sample filter, the light ~~attenuated~~ attenuates due to deposited particulate matter. The second filter, the reference filter, is located downstream the sample filter and allows blank filter reference light intensity measurements. ~~deposited on a quartz-fiber glass filter (PALL LifeScience, Pallflex Membrane Filters Type E70-2075W).~~

By default, the particle light absorption coefficient is determined internally using 60 s averages of the raw intensity measurements for both filter spots. Therefore, in Eq. (5) *I(t)* is defined as:

$$I(t) = \frac{I_{\mathrm{smp},\lambda}}{I_{\mathrm{ref},\lambda}}, \quad (7)$$

where I_{smp} and I_{ref} is the intensity of light at the certain wavelength λ behind the sample (smp) and blank reference (ref) filter, respectively. Nevertheless, all raw measurements are recorded with a time resolution of 1 Hz allowing a recalculation of σ_{abs} at this time resolution. The volumetric flow is set to one liter per minute (lpm). According to the manual, at an internal averaging interval of 60 s, the measurement uncertainty is specified to 0.2 Mm^{-1}. The spot diameter is ~4.8 mm which leads to a sample area of A_{spot} ~1.75e-5 m^2.

2.2.2 MA200

The second instrument used here is the microAeth® MA200 is a small sized (13.7 x 8.5 x 3.6 cm; 420g), absorption photometer measuring the attenuation of light at 5 wavelengths (375, 470, 528, 625, and 880 nm; 625 nm are investigated in this study) due to deposited particulate matter on a PTFE filter band.

Similarly to the STAP, the MA200 detects light intensities behind a sample and reference spot. The particulate matter samples on a sample spot with 3 mm diameter leading to a sample area of A_{spot} ~0.71e-5 m^2. The reference spot of same area allows for blank filter measurements. M_{eBC} is determined under the assumption that the change of attenuation is proportional to the deposited eBC mass. The measurements were recorded with a 1 Hz time resolution. With the DualSpot® technology the instrument is able to reduce uncertainties related to loading effects up to 60 % (Holder et al., 2018) but was not functioning at the time of the experiment.

Holder et al. (2018) reported that the measurements are slightly depending on *rh* and *T* of the aerosol sample. However, they observed concentrations of up to 7 mg m^{-3}, at which the observed dependence on humidity and temperature did not influence the measured values significantly. Furthermore, they used another version of the instrument (MA350), which may react differently to changes in humidity and temperature.

2.3 Experimental Set-up

The experimental setup is designed to examine the instrument filters in different states. Unloaded filters and differently loaded with black carbon and ammonium sulfate were investigated. The extent to which fast changes in the relative humidity of the air passing through the filter affect absorption measurements was investigated for these conditions. ~~In these states we investigated how fast changes of the relative humidity of the air flowing through the filters affect absorption measurements.~~

A miniCAST burner (model 5200, Jing Ltd.) was used to generate soot (black carbon; BC) aerosol particles due to combustion of propane. The produced BC particles stream can be diluted according the needs of the customer. A detailed description of the miniCAST is supplied by (Jing, 1999). Additionally, a solution of ammonium sulfate ($(NH_4)_2SO_4$; solution concentration of 0.05g/ 80 ml) was nebulized to an aerosol and was dried afterwards. Either the ammonium sulfate or the BC aerosol was fed into a 0.5 m^3 stainless steel mixing chamber. A fan within the chamber ~~with an included fan to~~ ensures a well-mixed ~~aerosol within the chamber~~aerosol.

The scheme of the experimental set up is described in Figure 1~~Figure 1~~. First, two particle free, dry (RH = 0%) air flows were produced. One of the flows was humidified by passing through two glass tubes containing distilled water at room temperature with an inlet and outlet for compressed particle free air. A maximum relative humidity of ~96% was reached. Both, the dry and humidified air flows were mixed together with a Swagelok brass T-shaped flow splitter and it was ensured that the sum of both mass-flows exceeded 1 lpm (controlled by a mass flow controller). Different *rh* were produced according to the ratios of the dry and humidified air. For this, valves with markings indicating the opening state ~~marks on the valves indicating the opening state~~ of the valve~~ss,~~ were used to reproduce consistent mixing *rh*. The *rh* and *T* of the airflow sampled

Formatiert: Schriftfarbe: Text 1, Englisch (USA)

with the photometer were detected with a temperature and relative humidity sensor (model HYT939, B+B Thermo-Technik GmbH, 78166 Donaueschingen, Germany) within an accuracy of ±1.8% (between 0 and 90% RH) and ±0.2°C (between 0 and 60°C). Furthermore, this sensor has a response time t_{63} of <10s. Additionally, this setup could be used with or without a silica bead-based dryer beforehand the photometers to examine to which extent a dryer dampens the effect of relative humidity changes on the photometer absorption measurements.

Two main setups were used to investigate the effect of changes in real humidity. In the first, the filters of the devices were unloaded and the instruments collected a particle free airflow with adjustable relative humidity to examine the pure filter effect. In the second, the filters of the devices are loaded to a certain degree and afterwards they sample particle-free humidified air which accounts for the combination of both effects, the pure filter effect and the effect induced by the hygroscopic behavior of the particles.

The ~~dried black carbon or ammonium sulfate~~loading aerosol was split into two streams from one of which ~~could be sampled on the photometer filters~~the absorption photometer were sampling simultaneously. The other one was sampled with a mobility particle sizer spectrometer (MPSS; working principle explained in e.g. Wiedensohler et al. (2012)) to measure the aerosol particle number size distribution from which the loading mass was estimated. An example of a generated ammonium sulfate aerosol is shown in Figure 2~~Figure 2~~. Furthermore, to examine the loading ~~the~~ mass concentration of the generated eBC (soot), the generated BC aerosol was measured also with a MAAP.

Formatiert: Schriftfarbe: Text 1

3 Results

This chapter will give an overview of the measurement results. The overall behavior of both instruments will be shown for wavelengths of 624 nm in the case of the STAP and 625 nm in the case of the MA200, respectively. A closer look at the behavior of both devices at 1 Hz time resolution shows that both devices differ greatly in quality (see Figure 3). The STAP (red dots and the smooth fit shown as black line) reacts very fast to relative humidity changes (drh/dt as purple line) and then returns relatively fast to the zero line. The MA200, on the other hand, also shows a fast response to relative humidity changes, but then shows a distinct exponential recovery (see Figure 3, blue dots and smooth fit shown as orange line) and reports absorption coefficients different from zero although there is no *rh* change.

Therefore, we use an averaging on a 60 second basis to describe the qualitative behavior of both devices. In the case of the STAP, the internal 60 second averaging is used. For the MA200, on the other hand, a 60-second "running average" is applied to the 1 Hz measurements.

The qualitative behavior of both devices is shown as follows. To each absolute change in the relative humidity (Δrh) the corresponding maximum of the excursion of the averaged absorption coefficient ($\Delta\sigma_{abs}$) has been assigned. Where the absolute change of the relative humidity is the difference between the relative humidity at the time of the largest excursion in the absorption coefficient and the relative humidity at the start of the excursion. This approach also excludes the response time of the *rh* sensor.

~~The particle light absorption coefficients in dependence of the absolute change in *rh* (Δrh) are the 60 second internal averaging readouts of the STAP and a 60 seconds floating average considering the MA200.~~ First, the results for the pure filter effect will be shown. ~~clean filters will be considered.~~ Afterwards, we present the results of the combined behavior of filter and aerosol particles on the filters. ~~for l~~For loaded filters, the combined effect will be shown separated into BC and ammonium sulfate loading ~~will be shown~~.

3.1 Clean filters

In Figure 4~~Figure 4~~, the time series of the measured *rh* upstream the two photometers (upper panel) and of σ_{abs} measured by the STAP (624 nm) and MA200 (625 nm) in the lower panel are shown. The air sampled by the photometers was entirely particle-free. Relative humidity was changed in this time series between 3.1 and 87.7 %. The change rate of *rh* (d*rh*/d*t*) was in the range of around -3.0 to 2.9 % s^{-1}. Whereas the measurements of the STAP ranging between -9.8 and 9.5 Mm^{-1} the ~~floating~~ running 60 s mean of the MA200 readouts were ranging from to 32.2 to -33.6 Mm^{-1}, respectively. Furthermore, Figure 4~~Figure 4~~ shows the opposing behavior of both instruments. Whereas the STAP reacts to positive change rates of the *rh* with positive particle light absorption coefficients, the MA200 measures negative particle light absorption coefficient and vice versa. Summarizing, this indicates that the different filter materials react opposing to each other.

Subramanian et al. (2008) observed that organic matter produced during low-temperature biomass burning has a liquid, bead-shaped appearance when collected on fibrous filter. Also, these organics can appear as translucent coatings on the filter fibers and therefore change significantly the interaction with incident light. Accordingly, for this study this means that the water in the collection stream can wrap itself around the filter fibers, analogous to the organic materials. Lack et al. (2008) has estimated the bias on filter-based absorption measurement due to loading with organic material. Under conditions with low mass concentrations of organic matter the agreement with photoacoustic-based aerosol light absorption measurements was 12 %. Whereas under conditions where the mass concentration of organic material was 15 to 20 times larger than that of light absorbing carbon, the difference was 50 – 80 %. Therefore the effect of coating with liquid matter around the fibers is not negligible. In the case of the STAP, the water beads and coating can lead to a higher net reflectance of the filter, which appears darker for the photodiode behind the filter. The instrument interprets this as an increased attenuation and hence as an increased absorption. In addition, the backing material consists of hydrophilic cellulose, which may absorb water under increased relative humidity and thus change its optical properties (Ogren et al., 2017). Compared to the fibrous structure of the quartz-fiber filter, ~~Whereas the~~ the PTFE filter of the MA200 is a porous, hydrophobic filter. We speculate that these properties result more into a collection of a thin ~~collects a small~~ film of water, which could act as an index matching between the refractive indices of the PTFE and air. An additional film with intermediate refractive index reduces the reflectance and thus increases the transmittance leading to a decreased attenuation. Hence, ~~T~~the instrument interprets decreases of the attenuation as negative absorption.

Since the filter in the STAP reveal positive and the filter in the MA200 a negative correlation to relative humidity changes a combination of both filters within one instrument could account for the observed effect. A new developed instrument could use these two different filter materials on two sampling spots to cancel out the effect of each other. Though, more

Formatiert: Schriftfarbe: Text 1

Formatiert: Schriftfarbe: Text 1

investigations have to be done, especially to understand the different recovery behaviors and effect magnitudes of the PTFE and quartz-fiber filter.

The overall behavior of both instruments in the case of clean filters is shown in Figure 5~~Figure 5~~ (upper left panel~~). Each point represents the corresponding maximum deviation of σ_{abs} ($\Delta\sigma_{abs}$) after the *rh* was changed. The amplitude of the relative humidity change was estimated by subtracting the starting *rh* at the start of the σ_{abs} excursion from the *rh* at the time of the maximum σ_{abs} deviation. Ongoing this will be referred as absolute *rh* change (Δrh)~~). For all investigated Δrh, the response behavior of the MA200 (R^2 = 0.99) is more stable than the STAP (R^2 = 0.78). However, the response is stronger than the average response of the STAP at the presented wavelength. Whereas the STAP shows a dependency of 0.14 Mm^{-1} $\%^{-1}$, which means an increase in absorption with increasing *rh*, the MA200, shows an opposing behavior with a larger absolute value in the slope of -0.41 Mm^{-1} $\%^{-1}$ (Appendixtable 1~~Appendixtable 1~~). As shown in Figure 5, for each device the magnitude of the deviation due to positive or negative changes in humidity is approximately the same.

Formatiert: Schriftfarbe: Text 1

3.2 Loaded filters

Different aerosol types deposit on the filter within the instruments while measuring σ_{abs}. These aerosol types are either hydrophilic or hydrophobic and hence experience water uptake or not under conditions of elevated *rh*. Hereby, the more particle material is deposited on the filter the more water deposits on the filter. Therefore, this section will show the influence of different filter loading materials on the *rh* effect and will also point out the effect of different filter loading mass. The observed effect will include both, the effect for clean filters (the pure filter effect) and the effect of the hygroscopic behavior of the particles loaded onto the filter. But, investigating the effect of the loading material alone is simply not possible since no filter material exist, which is not affected by *rh* changes. Therefore, the presented results are always a combination of the filter effect and the material effect. For both considered loading materials, the ~~Filter loading mass~~mass loaded onto the filters ~~is~~ was calculated by multiplying the ~~apparent~~ prevalent loading mass concentration within the mixing chamber ~~of the considered material~~ with the volume flow rate of the instrument and the loading duration. The filter were loaded to a certain extent with different materials and afterwards the absorption photometer were sampling particle free air with adjustable humidity. The different sample spot areas of the absorption photometers will be considered herein by normalizing the loaded mass with the respective sample spot area. Ongoing this will be referred as filter loading areal density ρ*.

3.2.1 Black carbon

During the experiment the eBC loading mass concentration was estimated with different methods depending on the stability of the mass concentration and loading duration and was ranging between 27.6 and 52.6 µg m^{-3}. In Table 1~~Table 1~~ ρ^* of eBC per spot area (ρ^*_{eBC}) of both instruments is shown. During experiment #1 (see Table 1) the mean absorption coefficient of the STAP was divided by a *MAC* of 6.6 m^2 g^{-1} since the absorption was stable during the loading period and it's a direct measure from the sampling instrument. For the experiment #2 the loading mass concentration was taken from the average of two consecutive MAAP measurements since the loading period was shorter than 2 minutes which is shorter than the internal

averaging period of the STAP so that no stable absorption coefficient readouts could be provided by the STAP. During experiment #3 no MAAP was available and the absorption coefficient measured by the STAP was unstable. We therefore decided to estimate the loaded eBC mass by integrating the absorption coefficient during the loading period and dividing it by the *MAC*. Four different ρ^*_{eBC} were considered in the case of the STAP, three for the MA200, respectively. Due to the smaller volume flow rate of the MA200, ρ^*_{eBC} is in each corresponding case smaller than ρ^*_{eBC} for the STAP and therefore, if any effects of different loadings are observed these might be not as distinct as for the STAP.

For all considered BC loading cases the averaged response of STAP and MA200 to relative humidity changes is shown in Figure 5~~Figure 5~~ (upper right panel) and corresponding linear fitting and correlation parameters are given in Appendixtable 1~~Appendixtable 1~~. The STAP shows a dependency of 0.29 Mm^{-1} $\%^{-1}$ in this case. This means absolute changes in *rh* affecting the BC loaded filter leading to stronger σ_{abs} deviations than in the clean case. For the MA200, the response of the instrument to rapid changes in *rh* does not depend on the loading material the filter with BC since the regression slope is the same as in the clean case. However, the y-intersects deviate from each other but within 0.6 Mm^{-1}. We assume that this could be due to the lower absolute loading on the filter (15% of the STAP loading because of 0.15 lpm flow rate compared to 1 lpm of the STAP) or the MA200 response is in general independent of the filter loading material.

Considering different loading areal densities, the MA200 shows more or less the same behavior (see Appendixtable 1~~Appendixtable 1~~ and Figure 7~~Figure 7~~).The slope of the linear correlation fit ranges from -0.42 Mm^{-1} $\%^{-1}$ to -0.37 Mm^{-1} $\%^{-1}$ for corresponding loading areal densities of 1.1 to 16.3 mg m^{-2}. The STAP shows a larger variability (Figure 7~~Figure 7~~, left panel, black and gray colors). For ρ^* of 2.8 to 42.9 mg m^{-2} the STAP response ranges from 0.17 Mm^{-1} $\%^{-1}$ to 0.62 Mm^{-1} $\%^{-1}$. However, these results may not be entirely representative since R^2 is only for a loading density of 13.7 mg m^{-2} larger than 0.9 (0.94). Maybe the smaller amount of data points in the other cases explains this. However, the number of data points observed with the MA200 was also small but R^2 is in each case larger than 0.9. Similar to the clean case, for both instruments, drying and humidifying the sample stream to the same extent resulted in a deviation of σ_{abs} with the similar magnitude.

Formatiert: Schriftfarbe: Text 1

Formatiert: Schriftfarbe: Text 1

Formatiert: Schriftfarbe: Text 1

3.2.2 Ammonia sulfate

The loading mass concentration of the ~~deposited~~ $(NH_4)_2SO_4$ aerosol depositing on the filters was estimated by integrating the mean ammonium sulfate aerosol particle volume size distribution of the loading period ~~of the generated ammonium sulfate particles~~ and multiplying thise volume concentration ~~of the ammonium sulfate aerosol during the loading period~~ (see Table 2~~Table 2~~) with an assumed ammonium sulfate density of 1.77 g cm^{-3} (Haynes, 2014). The loading mass concentrations were in the range of 27.2 to 59.3 µg m^{-3} (see Table 2~~Table 2~~). The very narrow standard deviation around the mean particle number and volume size distribution in Figure 2 indicate clearly that the loading mass concentrations were very stable during the loading periods.

In the experiments ammonium sulfate filter loading areal densities were 3.1 to 99.6 mg m^{-2} in the case of the STAP and 1.2 to 15.9 mg m^{-2} in the case of the MA200. Exemplarily, PNSD and PVSD of the ammonium sulfate aerosol of the

loading on Feb. 23 are shown in Figure 2~~Figure 2~~. It is clearly visibly that the ammonium maximum in the particle volume size distribution peaked around a mobility diameter of 260 nm.

Figure 6~~Figure 6~~ shows exemplarily the time series of ~~*rh* of~~ the sample~~d~~ air *rh* and of the σ_{abs} measured with STAP and MA200 operated with clean filters. A *rh* of 0.0 to 96.2% with ~~d*rh*/d*t*~~ humidity change rates of ~~in the range of~~ -1.42 ~~and~~ to 1.09 % s^{-1} was measured. Compared to the case in Figure 4~~Figure 4~~ here a step-wise change of *rh* is shown. These steps resulted in a smaller absolute excursion of σ_{abs} which ranges from -7.2 to 9.0 Mm^{-1} (STAP; 624 nm, 60 s measurement resolution) and -14.1 to 10.9 Mm^{-1} (MA200; 625 nm, 60 second ~~floating~~ running mean). Furthermore, Figure 6 shows the response of the σ_{abs} to *rh* changes at three different states of filter loading. During the first ramp the filter were clean, during the second period the filters had a filter areal loading density of 32.5 (STAP) and 12.4 (MA200) mg m^{-2} and during the third ramp the filter in the STAP had loading areal density of 98.7 mg m^{-2} and the MA200 filter was loaded with an areal loading density of 37.6 mg m^{-2}. The response of the instruments during these periods is shown in Appendixtable 1~~Appendixtable 1~~.

In Figure 5~~Figure 5~~ (lower left panel), the overall (mean) response of both instruments to *rh* changes is shown in the case of loading with ammonium sulfate. The MA200 behaves similarly to the clean and BC case (slope of -0.40 Mm^{-1} $\%^{-1}$). The σ_{abs} measured by the STAP responses ~~the opposite way~~opposingly with a positive slope of 0.21 ± 0.01 Mm^{-1} $\%^{-1}$ which is roughly half ~~of~~ the amplitude~~response of~~ shown by the MA200 and around two thirds of the BC loaded case.

As shown in Figure 6, both absorption photometers measure an "apparent" absorption coefficient of approximately 2 Mm^{-1} during loading with ammonium sulfate (18:30 and 21:00 UTC). This shows that absorption photometers react sensitively to scattering aerosols such as ammonium sulfate. The scattering ability of any material can be described with the real part of its refractive index. It seems that for the STAP the slope of the correlation increases with increasing scattering of the loading material (0.15 Mm^{-1} $\%^{-1}$ for a clean filter, 0.21 Mm^{-1} $\%^{-1}$ for ammonium sulfate, and 0.30 Mm^{-1} $\%^{-1}$ for BC). Ammonium sulfate has a real part of 1.521 ± 0.002 (at 532 nm Dinar et al, 2007) and BC from combustion processes has a real part of 1.96 at 530 nm (Kim et al., 2015 following Ackermann and Toon (1981)). Hence, the quartz fiber glass filters loaded with "artificially" absorbing aerosol inside the STAP could lead to a variation in the response to relative humidity changes. But, the MA200 was loaded with ammonium sulfate as well and its response to relative humidity changes is almost constant for all considered loading materials. Therefore, either the observation is caused by the interaction of quartz fiber glass filters with the loading material and the PTFE filter inside the MA200 do not causes this behavior, the filter loading of the MA200 was too low, or there are other mechanisms explaining this. Furthermore, since only three different cases (clean, ammonium sulfate and BC) were observed in this study more materials should be considered to investigate this phenomenon. ~~It seems that for the STAP the slope of the correlation increases with increasing imaginary part of the loading material (0.15 Mm^{-1} $\%^{-1}$ for a clean filter, 0.21 Mm^{-1} $\%^{-1}$ for ammonium sulfate with an imaginary part of i0.002 ± 0.002 (at 532 nm Dinar et al, 2007) or i6.361e-8 (at 550 nm and 40 % *rh*; Erlick et al, 2011), and 0.30 Mm^{-1} $\%^{-1}$ for BC with an imaginary part of i0.65 at 530 nm (Kim et al., 2015 following Ackermann and Toon (1981)). Three different cases were observed in this study only so that more materials should be considered to confirm or neglect this theory.~~

Formatiert: Schriftfarbe: Text 1

Formatiert: Schriftfarbe: Text 1

Formatiert: Schriftfarbe: Text 1

Formatiert: Schriftfarbe: Text 1

No correlation of linear regression slope and filter loading areal density ρ^* was observed in either case, for the STAP and the MA200, respectively. The slope (a) of STAP ranges from 0.17 Mm^{-1} $\%^{-1}$ to 0.24 Mm^{-1} $\%^{-1}$, and from -0.36 Mm^{-1} $\%^{-1}$ to -0.42 Mm^{-1} $\%^{-1}$ for the MA200. With a relative difference from minimum to maximum slope of 15.2 % the response of the MA200 is less variable than of the STAP with a relative variability of 28.6 % (slopes with $R^2 < 0.8$ excluded, all points included 36.8%). In Figure 7~~Figure 7~~ (middle panel),~~T~~ the spread of the slopes within the shown cases is exemplarily shown for the investigated minimum and maximum load of the filters~~. in Figure 6 (middle panel)~~. Overall, the magnitude of the deviation of σ_{abs} was independent of the sigh of humidity change for both instruments.

Formatiert: Schriftfarbe: Text 1

3.3 Correction approach

The above chapters describe the overall behavio~~u~~r of the instruments to relative humidity changes averaging time of for 60 seconds. To correct for the described effect 1 Hz time resolution is needed to resolve the instantaneous response of the instruments to relative humidity changes. For this purpose, a further laboratory experiment was conducted in which the inlets of both instruments could be flexibly exposed to humidified air. In our particular case, we hold the inlet into a beaker with a moistened tissue. In order to avoid any dampening bias ~~by a filter~~, all measurements were conducted without particle filter in front of the inlet. But, during this experiment ~~under relatively clean laboratory conditions with~~ a background of about σ_{abs} of 1.2 Mm^{-1} was measured so that the filter loading was very low. First we will consider the STAP and afterwards the MA200 is investigated.

3.3.1 STAP

In Figure 8~~Figure 8~~ the correlation of rh change rate (drh/dt) and the measured σ_{abs} at 624 nm measured by the STAP (red circles) and recalculated with respect to standard conditions (pressure of 1013.25 hPa and temperature 273.15 K) is shown. The STAP-based background eBC mass concentration during the experiment was ~190 ng m^3 (at standard conditions, σ_{abs} at 624 nm converted with a MAC of 6.6 m^2 g^{-1}), which corresponds to offset (standard conditions corrected values) in the shown scatterplot of Figure 8~~Figure 8~~ and which has no influence on the response to rh changes as shown previously.

Formatiert: Schriftfarbe: Text 1

Formatiert: Schriftfarbe: Text 1

The rh change rate ranged from -10.8 to 14.5 % s^{-1}. These rates correspond to a σ_{abs} of -231 to 192 Mm^{-1} for recalculated values at standard conditions and -203 to 164 Mm^{-1} directly measured by the instrument. But these measurements are biased by the response time of the relative humidity sensor so that the "real" rh change-rate cannot fully represented by these measurements. On average the slope (correction factor C_{rh} in Eq. (~~7~~8)) of the linear fit is 10.08 (± 0.12) Mm^{-1} s $\%^{-1}$ for standard conditions and 8.82 (± 0.10) Mm^{-1} s $\%^{-1}$ for direct instrument output, respectively. Calculating the particle light absorption coefficient introduced by rh changes with:

$$\sigma_{abs,rh} = C_{rh} \frac{drh}{dt}, \quad (8)$$

~~$\sigma_{abs,rh} = C_{rh} \cdot drh/dt$~~ for different rh change rates in both, the recalculated and direct instrument output case, and subtracting it from measurements allows to correct for the observed effect as follows:

$$\sigma_{\mathrm{abs,corr}} = \sigma_{\mathrm{abs,meas}} - \sigma_{\mathrm{abs,rh}} \quad (7\,9)$$

and after replacing $\sigma_{\mathrm{abs,rh}}$ in Eq. (8) with Eq. (9) follows:

$$\sigma_{\mathrm{abs,corr}} = \sigma_{\mathrm{abs,meas}} - C_{\mathrm{rh}} \frac{\mathrm{d}rh}{\mathrm{d}t}. \quad (10)$$

The y-intersect of the linear fit in Figure 8~~Figure 8~~ has not to be considered for correction as mentioned before. Disadvantageously, with this correction the noise of the *rh* sensor will propagate in the corrected σ_{abs}. Furthermore, the linear fit in Figure 8~~Figure 8~~ under- or overestimates the behavior in regimes of very high relative humidity change rates most likely due to the response time of the *rh* sensor, so that ~~in these cases~~ the correction function cannot entirely correct the bias. Therefore, the given correction factor C_{rh} consists of uncertainties, which cannot be entirely addressed. Hence, it is only a first guess, needs further refinement and right now we do not recommend to use the correction approach as long the uncertainties are not fully addressed. Furthermore, since only one STAP was tested, other STAP may have other correction factors due to a unit to unit variability. Additionally, other filter materials used in the STAP can also lead to another behavior. Anyhow, t~~T~~he upper function ~~can be~~ was applied ~~since the~~to STAP measurements conducted with the same *rh* sensor under atmospheric conditions. ~~instantaneously reacts to *rh* changes and immediately shows the unbiased σ_{abs}, when no change in *rh* is prevalent. Disadvantageously, with this correction the noise of the *rh* sensor will propagate in the corrected σ_{abs}. Furthermore, the linear fit in Figure 8 under- or overestimates the behavior in regimes of very high relative humidity change rates, so that in these cases the correction function cannot entirely correct the bias. Furthermore, since only one STAP was tested, other STAP may have other correction factors due to unit to unit variability. Additionally, other filter materials used in the STAP can also lead to another behavior.~~

Exemplarily, Figure 9~~Figure 9~~ shows this application. ~~of the correction function for STAP measurements.~~ The figure shows airborne measurements of σ_{abs} at 624 nm derived with the STAP derived during a campaign conducted in March 2017 in East Germany. The upper panel displays the *rh* of a dried aerosol sample stream measured upstream of the STAP. The lower panel shows the recalculated σ_{abs} at 624 nm wavelength corrected for *rh* changes (black) and biased by *rh* changes (red). In the periods where the *rh* changes relatively fast (d*rh*/d*t* of -0.55 to 0.56 % s^{-1} e.g. at around 6200 seconds), the uncorrected σ_{abs} overshoots. The correction significantly reduces this bias and smooth out the measurements during the periods of *rh* changes. At the peaks of d*rh*/d*t* the difference of the corrected and uncorrected values is up to 1.5 Mm^{-1}, which is significant with respect to the measured σ_{abs}. The periods with negative σ_{abs} are not introduced by the *rh* effect. We moreover think that a small offset is introduced in the initialization process of the instrument. Despite the imperfection of the correction scheme, this linear approach can be useful to derive a rough estimate of the accuracy of the measurements. For instance let *x* be the required accuracy for the measurements in % and σ_{abs} the measured particle light absorption coefficient we can express the ambient particle light absorption coefficient which is at least needed to fulfill the accuracy criterion in dependency of the *rh* change rate d*rh*/d*t*:

Formatiert: Schriftfarbe: Text 1

Formatiert: Schriftfarbe: Text 1

$$\sigma_{abs,meas} \geq \frac{100\%}{x[\%]} C_{rh} \left[\frac{Mm^{-1}s}{\%}\right] \left|\frac{drh}{dt}\right| \left[\frac{\%}{s}\right]. \quad (11)$$

Exemplarily, if a change rate of 0.1 % s^{-1} is measured and an accuracy of 25% is needed, at least a measured particle light absorption coefficient of around 4 Mm^{-1} is needed to fulfill the accuracy criterion.

3.3.2 MA200

~~Whereas the STAP shows a linear response to *rh* changes, the MA200 is more complex and shows an exponential decay after it got exposed to *rh* changes~~The exponential recovery behavior of the MA200 (see Figure 3) requires a more complex approach to correct for relative humidity changes. Therefore, the "apparent" particle light absorption coefficient can be described as a function of d*rh*/d*t* at a given time *t* ($\sigma_{abs,rh,t}$):

$$\sigma_{abs,rh,t} = a\frac{drh}{dt} + b\sigma_{abs,rh,t-1}, \quad (12~~8~~)$$

with *a* is a linear factor describing the dependency of $\sigma_{abs,rh}$ to d*rh*/d*t* and *b* is an exponential decay parameter between 0 and 1. The Eq. (~~8~~12) corresponds to an autoregressive moving average model with exogenous variable (ARMA-X).

The function *marima* of the *R* package *marima* (v2.2) is capable to derive such an ARMA-X model (details in Appendix A). From this the coefficients *a* and *b* can be derived. These can be furthermore used as initial parameters for an optimization by minimizing the sum of the squared residual errors ~~squared~~. The derived ARMA-X model describes σ_{abs}(d*rh*/d*t*) as follows:

$$\sigma_{abs,rh}(t) = -0.47\left[\frac{Mm^{-1}s}{\%}\right]\frac{drh}{dt}(t) + 0.93\sigma_{abs,rh}(t-1), \quad (~~9~~13)$$

and with the applied optimization:

$$\sigma_{abs,rh}(t) = -0.50\left[\frac{Mm^{-1}s}{\%}\right]\frac{drh}{dt}(t) + 0.96\sigma_{abs,rh}(t-1). \quad (~~10~~14)$$

~~Figure 10~~Figure 10 shows time series of *rh* (upper panel) and 60 s ~~floating~~ running average σ_{abs} derived with the MA200 at 625 nm with 1 Hz time resolution derived during the laboratory experiment mentioned in 3.4. Under the influence of d*rh*/d*t* in the range of -11.2 to 17.1 % s^{-1} the 60 s ~~floating~~ running average of σ_{abs} is between -6.5 to 7.7 Mm^{-1} (M_{eBC} equivalent of -0.99 to 1.20 µg m^{-3}). Subtracting the calculated "apparent" particle light absorption coefficient in dependency of *rh* changes following Eq. (~~9~~13) and (~~10~~14) to this data set σ_{abs} shrinks to -3.2 to 4.7 Mm^{-1} or -1.0 to 3.7 Mm^{-1} in the non- and optimized case, respectively. This corresponds to M_{eBC} of around -0.5 to 0.7 µg m^{-3}, or -0.2 to 0.6 µg m^{-3} in the optimized case. This indicates, that the presented approach can significantly reduce the *rh* bias in the presented case. But, *rh* change induced fluctuations in σ_{abs} are still visible, which indicates that correction scheme cannot account entirely for all the bias introduced

Formatiert: Schriftfarbe: Text 1

by a change in *rh*. Here, the response time of the sensor could account at least for a part of the imperfection of the correction approach and cannot be fully quantified, yet.

Unfortunately, the application of the same correction approach to other similar experiments resulted in different correction function *a* and *b*. Applying the approach to two clean case experiments from section 3.1 resulted in optimized parameters of *a* = -0.92 and -1.03 and *b* = 0.974 and 0.971, respectively. Hence, it is just a first step trying to account for relative humidity changes and further research with more MA200 simultaneously has to be done to fully understand the underlying processes and to fully quantify the uncertainties of the correction scheme~~.~~ Nevertheless, the presented approach significantly reduces the amplitude of the bias in the shown data set (see Figure 10~~Figure 10~~). But, up to now we cannot recommend to use the given parameters to correct for *rh* effects. At most it can be used to make a rough estimate of how measurements of the particle light absorption coefficient derived the MA200 could be biased by *rh* changes.

Formatiert: Schriftfarbe: Text 1

6 Summary and Conclusion

Here we presented a unique set of laboratory studies to investigate the response of two different types of filter-based absorption photometers (STAP and MA200) with different filter material (quartz-fiber glass, and PTFE) to relatively fast changes in relative humidity of sampled aerosol. Different filter loading densities with different loading material (clean, black carbon, and ammonium sulfate) where considered in this study. Both instruments revealed that they react to fast humidity changes but in opposite ways, induced by the different filter material. This opposing behavior could be a chance to design an instrument on the basis of both filter materials so that the effects cancel out each other. No significant differences between the loading aerosol types were observed in the case of the MA200, whereas the STAP revealed the strongest response in the BC case. ~~Furthermore, we investigated the effect of drying the airstream (aerosol) beforehand. Installing a dryer upstream reduced the excursion significantly, because the absolute excursion of the prevalent was reduced more than two times in amplitude.~~

The MA200 revealed a very robust response of -0.42 to -0.36 Mm^{-1} $\%^{-1}$ (negative excursion of σ_{abs} with increasing *rh*), whereas the STAP was more fluctuating across loading areal density and loading aerosol type with a positive excursion of σ_{abs} in the range of 0.17 to 0.62 Mm^{-1} $\%^{-1}$. We assume that in the case of the MA200 it is more a filter effect, or the filter loadings were too low to have a significant effect due to the lower volume flow rate. For the STAP, more parameters could also have an effect and further investigation is needed. For loading areal density on the filter no correlation was found, although we expected that the hygroscopic ammonium sulfate will affect the transmissivity of the filter-aerosol layer. Hence, we think excursions of σ_{abs} due to relative humidity changes is mainly caused by water vapor filter material interactions and is independent of the filter loading areal density or they were too low to observe significant effects.

Furthermore, we developed some correction approaches for both instruments to account for fast *rh* changes. For the STAP a linear correction function ~~could be provided~~was derived. This correction follows a linear approach including a correction factor of C_{rh} = 10.08 ± 0.12 Mm^{-1} s $\%^{-1}$ for standard conditions and 8.82 ± 0.10 Mm^{-1} s $\%^{-1}$ for direct instrument output without any corrections. ~~Exemplarily, this correction was applied to an airborne data set and has shown promising~~

~~results.~~ But this correction was created with a *rh* sensor with a response time which introduces a bias in the correction approach and cannot be quantified, yet. Also, other *rh* sensors might result in a different correction formula. Exemplarily, this correction was applied to an airborne data set and has shown promising results. For the MA200 no linear correction function can be provided, since after an excursion of σ_{abs} the MA200 shows a~~n~~ distinct exponentially behaving recovery function. Therefore an ARMA-X model was developed to account for this exponential decay and to describe the σ_{abs} in dependency of d*rh*/d*t*. Applying this to the presented data set, this significantly reduced the excursion introduced by *rh* changes. ~~But, the~~We do not recommend to use the presented approach~~es cannot be applied yet~~, since the uncertainties cannot be fully quantified yet and a refinement is need ~~and has to be derived~~ on the base of more experiments to fully understand the underlying processes and to quantify the uncertainties.

~~Recommendations~~

The findings summarized above lead to following recommendations how to use this type of instruments:

1. When used for vertical profiling, apparent sharp gradients in *rh* during the profile have to be taken into account.
    a. The ascending speed of the profiling platform should be reduced if possible, to decrease the temporal change of *rh*, but in some scenarios this is simply not possible and therefore,
    b. when fast relative humidity changes cannot be avoided, such periods have to be removed from the data set, or at least to estimate the uncertainties of the measurements based on the presented correction functions. Therefore,
2. we recommend recording the *rh* of the sampled aerosol. This allows to determine *rh* change rates. This allows to roughly estimate the bias of *rh* changes on filter-based absorption measurements with these two instruments.
3. The usage of a dryer is highly recommended, because it reduces the amplitude of the excursion in the measurements during fast *rh* changes.
4. For both instruments we recommend to conduct more similar experiments to address the flaws of our study to refine the presented correction approaches.
5. Since the response is different in magnitude and sign for both filter materials, we recommend to examine the effect for other filter materials as well.

Appendix A: Multivariate Autoregressive Integrated Moving Average model with exogenous variable – MARIMA-X

The multivariate autoregressive integrated moving average model with exogenous variable (MARIMA-X(p,d,q)) can model the behaviour of an observation driven by an exogenous variable. It consists of three parts, the autoregressive (AR) part of order p, the moving average (MA) part of order q, and the integrating (I) part, which describes how often (*d* times) a time series must differentiated to be stationary. An MARIMA-X model can be described as:

$$Y_t = aX_t + b_1Y_{t-1} + b_2Y_{t-2} + \ldots + b_nY_{t-n} + \epsilon_t + c_2\epsilon_{t-2} + c_1\epsilon_{t-1} + \ldots + c_n\epsilon_{t-n}, \quad \text{(A1)}$$

with Y_t the predicted value of the model at the time *t*. b_1Y_{t-1} to b_nY_{t-n} are part of the autoregressive module of the model, with the corresponding coefficients b_1 to b_n, describing the contribution of each Y_{t-n} to Y_t. X_t represents the corresponding independent exogenous variable at time *t*, whereas the ϵ_t are part of the moving average of the model, which accounts for lagged error terms, ϵ_t introduced by the model itself. c_1 to c_n indicate the contribution of ϵ_t to ϵ_{t-n} to Y_t. For predictions of a variable the error term is unknown. A special case of the MARIMA-X model is the MARMA-X model or ARMA-X, in which the integrating part has an order of 0. Detailed informations about ARIMA models can be found in Durbin and Koopman (2012) and Lütkepohl (2005). A tutorial to estimate MARIMA models in *R* is provided by Spliid (2016).

Appendix B: Table with overview of all investigated cases

Acknowledgements

We would like to thank Dr. Sascha Pfeiffer very much for his guidance in setting up the experiment and for the introduction to the particle generators. We would also like to express our sincere thanks to Ralf Käthner for his valuable support with data acquisition troubleshooting.

References

Ackerman, T. P., and Toon, O. B.: Absorption of Visible Radiation in Atmosphere Containing Mixtures of Absorbing and Non-Absorbing Particles, Appl. Opt., 20, 3661–3668, 1981.

Alas, H.D., Müller, T., Birmili, W., Kecorius, S., Cambaliza, M.O., Simpas, J.B.B., Cayetano, M., Weinhold, K., Vallar, E., Galvez, M.C. and Wiedensohler, A.: Spatial characterization of black carbon mass concentration in the atmosphere of a Southeast Asian megacity: An air quality case study for Metro Manila, Philippines. Aerosol Air Qual. Res. 18: 2301–2317, 2018.

Bärfuss, Konrad; Pätzold, Falk; Altstädter, Barbara; Kathe, Endres; Nowak, Stefan; Bretschneider, Lutz; Bestmann, Ulf; Lampert, Astrid: New Setup of the UAS ALADINA for Measuring Boundary Layer Properties, Atmospheric Particles and Solar Radiation. In: Atmosphere 9, p. 28, 2018.

B+B Thermo-Technik GmbH, HYT-939 data-sheet, url: https://shop.bb-sensors.com/out/media/Datasheet_digital_humidity_sensor_HYT939.pdf, 2015

Birmili, W., Weinhold, K., Rasch, F., Sonntag, A., Sun, J., Merkel, M., Wiedensohler, A., Bastian, S., Schladitz, A., Löschau, G., Cyrys, J., Pitz, M., Gu, J., Kusch, T., Flentje, H., Quass, U., Kaminski, H., Kuhlbusch, T. A. J., Meinhardt, F., Schwerin, A., Bath, O., Ries, L., Gerwig, H., Wirtz, K., and Fiebig, M.: Long-term observations of tropospheric particle number size distributions and equivalent black carbon mass concentrations in the German Ultrafine Aerosol Network (GUAN), Earth Syst. Sci. Data, 8, 355-382, https://doi.org/10.5194/essd-8-355-2016, 2016.

T. C. Bond, T. L. Anderson & D. Campbell: Calibration and Intercomparison of Filter-Based Measurements of Visible Light Absorption by Aerosols, AerosolScience & Technology, 30:6, 582-600, DOI: 10.1080/027868299304435, 1999.

T. C. Bond, S. J. Doherty, D. W. Fahey, P. M. Forster, T. Berntsen, B. J. DeAngelo, M. G. Flanner, S. Ghan, B. Kärcher, D. Koch, S. Kinne, Y. Kondo, P. K. Quinn, M. C. Sarofim, M. G. Schultz, M. Schulz, C. Venkataraman, H. Zhang, S. Zhang, N. Bellouin, S. K. Guttikunda, P. K. Hopke, M. Z. Jacobson, J. W. Kaiser, Z. Klimont, U. Lohmann, J. P. Schwarz, D. Shindell, T. Storelvmo, S. G. Warren, C. S. Zender (2013), Bounding the role of black carbon in the climate system: A scientific assessment, J. Geophys. Res. Atmos., 118, 5380–5552, doi:10.1002/jgrd.50171, 2013.

Cai, J., Yan, B., Ross, J., Zhang, D., Kinney, P. L., Perzanowski, M. S., Chillrud, S. N.: Validation of microAeth® as a black carbon monitor for fixed-site measurement and optimization for personal exposure characterization. Aerosol and Air Quality Research, 14(1), 1–9. https://doi.org/10.4209/aaqr.2013.03.0088, 2014.

Caroll, B. J.: The accurate measurement of contact angle, phase contact areas, drop volume, and Laplace excess pressure in drop-on-fiber systems, J. Coll. Interface Sci., 57(3), 488-495, 1976.

Caroll, B. J.: Equilibrium conformations of liquid drops on thin cylinders under forces of capillarity. A theory for the roll-up process., Langmuir, 2(2), 248-250, 1986.

Cepeda, M., Schoufour, J., Freak-Poli, R., Koolhaas, C., Dhana, K., Bramer, W. and Franco, O.: Levels of ambient air pollution according to mode of transport: a systematic review. *The Lancet Public Health*, 2(1), pp.e23-e34, 2017.

Dinar, E., Abo Riziq, A., Spindler, C., Erlick, C., Kiss, G., & Rudich, Y.: The complex refractive index of atmospheric and model humic-like substances (HULIS) retrieved by a cavity ring down aerosol spectrometer (CRD-AS), Faraday Discussions, 137, 275-295, https://doi.org/10.1039/b703111d, 2007.

Durbin, J. and Koopman, S.: Time series analysis by state space methods. Oxford: Oxford University Press, 2012.

~~Erlick, C., Abbatt, J. P. D., & Rudich, Y.: How Different Calculations of the Refractive Index Affect Estimates of the Radiative Forcing Efficiency of Ammonium Sulfate Aerosols. Journal of the Atmospheric Sciences, 68(9), https://doi.org/10.1175/2011JAS3721.1, 2011.~~

Ferrero, L., Castelli, M., Ferrini, B. S., Moscatelli, M., Perrone, M. G., Sangiorgi, G., D'Angelo, L., Rovelli, G., Moroni, B., Scardazza, F., Močnik, G., Bolzacchini, E., Petitta, M., and Cappelletti, D.: Impact of black carbon aerosol over Italian basin valleys: high-resolution measurements along vertical profiles, radiative forcing and heating rate, Atmos. Chem. Phys., 14, 9641-9664, https://doi.org/10.5194/acp-14-9641-2014, 2014

Ferrero, L., Cappelletti, D., Busetto, M., Mazzola, M., Lupi, A., Lanconelli, C., Becagli, S., Traversi, R., Caiazzo, L., Giardi, F., Moroni, B., Crocchianti, S., Fierz, M., Močnik, G., Sangiorgi, G., Perrone, M. G., Maturilli, M., Vitale, V., Udisti, R., and Bolzacchini, E.: Vertical profiles of aerosol and black carbon in the Arctic: a seasonal phenomenology along 2 years (2011–2012) of field campaigns, Atmos. Chem. Phys., 16, 12601-12629, https://doi.org/10.5194/acp-16-12601-2016, 2016.

Haynes, W.M. (ed.). CRC Handbook of Chemistry and Physics. 95th Edition. CRC Press LLC, Boca Raton: FL 2014-2015, 2014.

Holder, A., B. Seay, A. Brashear, T. Yelverton, J. Blair, and S. Blair. Evaluation of a multi-wavelength black carbon sensor, Poster, 10th International Aerosol Conference, St. Louis, MO, September 02 - 07, url: https://cfpub.epa.gov/si/si_public_record_report.cfm?Lab=NRMRL&dirEntryId=342614, 2018.

IPCC: Cubasch, U., D. Wuebbles, D. Chen, M.C. Facchini, D. Frame, N. Mahowald and J.-G. Winther: Introduction. In: Climate Change 2013: The Physical Science Basis. Contribution of Working Group I to the Fifth Assessment Report of the Intergovernmental Panel on Climate Change [Stocker, T.F., D. Qin, G.-K. Plattner, M. Tignor, S.K. Allen, J. Boschung, A. Nauels, Y. Xia, V. Bex and P.M. Midgley (eds.)]. Cambridge University Press, Cambridge, United Kingdom and New York, NY, USA, 119–158, doi:10.1017/CBO9781107415324.007., 2013.

Jing, L.: Standard Combustion Aerosol Generator for Calibration Purposes. 3rd ETH Conference on Combustion Generated Nanoparticles. Zurich, 9–10 August, 1999.

Kim, J., Bauer, H., Dobovičnik, T., Hitzenberger, R., Lottin, D., Ferry, D., & Petzold, A.: Assessing optical properties and refractive index of combustion aerosol particles through combined experimental and modeling studies. Aerosol Science and Technology, 49(5), 340-350, https://doi.org/10.1080/02786826.2015.1020996, 2015.

Lack, D. A., Cappa, C. D., Covert, D. S., Baynard, T., Massoli, P., Sierau, B., Bates, T. S., Quinn, P. K., Lovejoy, E. R., & Ravishankara, A. R.: Bias in Filter-Based Aerosol Light Absorption Measurements Due to Organic Aerosol Loading: Evidence from Ambient Measurements, Aerosol Science and Technology, 42:12, 1033-1041, DOI: 10.1080/02786820802389277, 2008.

Lütkepohl H.: Introduction To Multiple Time Series Analysis, Berlin: Springer-Verlag; 2005.

Markowicz, K. M., Ritter, C., Lisok, J., Makuch, P., Stachlewska, I. S., Cappelletti, D., Chilinski, M. T.: Vertical variability of aerosol single-scattering albedo and equivalent black carbon concentration based on in-situ and remote sensing techniques during the iAREA campaigns in Ny-Ålesund. Atmospheric Environment. https://doi.org/10.1016/j.atmosenv.2017.06.014, 2017.

Nessler, R., Sheridan, P.J., Ogren, J.A., Weingartner, E., and Hannemann, A.: Effect of humidity on filter-based measurements of the aerosol light absorption. NOAA ESRL GLOBAL MONITORING ANNUAL CONFERENCE, 2006.

Ogren, J. A., Wendell, J., Andrews, E., and Sheridan, P. J.: Continuous light absorption photometer for long-term studies, Atmos. Meas. Tech., 10, 4805-4818, https://doi.org/10.5194/amt-10-4805-2017, 2017.

Ogren, J.A.: Comment on “Calibration and Intercomparison of Filter-Based Measurements of Visible Light Absorption by Aerosols”, Aerosol Science and Technology, 44:8, 589-591, DOI: 10.1080/02786826.2010.482111, 2010.

Petzold, A. and M. Schönlinner: Multi-angle absorption photometry – a new method for the measurement of aerosol light absorption and atmospheric black carbon, *J. Aerosol Sci.*, 35, 421-441, 2004.

Petzold, A., Ogren, J. A., Fiebig, M., Laj, P., Li, S.-M., Baltensperger, U., Holzer-Popp, T., Kinne, S., Pappalardo, G., Sugimoto, N., Wehrli, C., Wiedensohler, A., and Zhang, X.-Y.: Recommendations for reporting "black carbon" measurements, Atmos. Chem. Phys., 13, 8365-8379, https://doi.org/10.5194/acp-13-8365-2013, 2013.

Ran, L., Deng, Z., Xu, X., Yan, P., Lin, W., Wang, Y., Tian, P., Wang, P., Pan, W., and Lu, D.: Vertical profiles of black carbon measured by a micro-aethalometer in summer in the North China Plain, Atmos. Chem. Phys., 16, 10441–10454, https://doi.org/10.5194/acp-16-10441-2016, 2016.

Rosati, B., Herrmann, E., Bucci, S., Fierli, F., Cairo, F., Gysel, M., Tillmann, R., Größ, J., Gobbi, G. P., Di Liberto, L., Di Donfrancesco, G., Wiedensohler, A., Weingartner, E., Virtanen, A., Mentel, T. F., and Baltensperger, U.: Studying the vertical aerosol extinction coefficient by comparing in situ airborne data and elastic backscatter lidar, Atmos. Chem. Phys., 16, 4539-4554, https://doi.org/10.5194/acp-16-4539-2016, 2016.

Spliid, H.: Multivariate Time Series Estimation using marima. In . P. Linde (Ed.), Symposium i anvendt statistik 2016 (pp. 108-123). Danmarks Statistik, 2016.

Subramanian, R., Roden, C. A., Boparai. P., and Bond, T. C.: Yellow Beads and Missing Particles: Trouble Ahead for Filter-Based Absorption Measurements, Aerosol Sci. Technol. 41:6, 630–637, https://doi.org/10.1080/02786820701344589, 2007.

Telg, H., Murphy, D. M., Bates, T. S., Johnson, J. E., Quinn, P. K., Giardi, F., and Gao, R.: A practical set of miniaturized instruments for vertical profiling of aerosol physical properties, Aerosol Science and Technology, 51:6, 715-723, DOI: 10.1080/02786826.2017.1296103, 2017.

Vecchi, R., Bernardoni, V., Paganelli, C., and Valli, G..: A filter-based light-absorption measurement with polar photometer: Effects of sampling artefacts from organic carbon, Journal of Aerosol Science., 70, 4805-4818, https://doi.org/10.1016/j.jaerosci.2013.12.012, 2013.

Wiedensohler, A., Birmili, W., Nowak, A., Sonntag, A., Weinhold, K., Merkel, M., Wehner, B., Tuch, T., Pfeifer, S., Fiebig, M., Fjäraa, A. M., Asmi, E., Sellegri, K., Depuy, R., Venzac, H., Villani, P., Laj, P., Aalto, P., Ogren, J. A., Swietlicki, E., Williams, P., Roldin, P., Quincey, P., Hüglin, C., Fierz-Schmidhauser, R., Gysel, M., Weingartner, E., Riccobono, F., Santos, S., Grüning, C., Faloon, K., Beddows, D., Harrison, R., Monahan, C., Jennings, S. G., O'Dowd, C. D., Marinoni, A., Horn, H.-G., Keck, L., Jiang, J., Scheckman, J., McMurry, P. H., Deng, Z., Zhao, C. S., Moerman, M., Henzing, B., de Leeuw, G., Löschau, G., and Bastian, S.: Mobility particle size spectrometers: harmonization of technical standards and data structure to facilitate high quality long-term observations of atmospheric particle number size distributions, Atmos. Meas. Tech., 5, 657-685, https://doi.org/10.5194/amt-5-657-2012, 2012.

World Health Organization (European Office): Health Effects of Black Carbon. Copenhagen, Denmark: WHO, ISBN: 9789289002653 2012.

WMO/GAW: Aerosol measurement procedures guidelines and recommendations 2nd edition, GAW Rep. 227, World Meteorol. Organ., Geneva, Switzerland, https://library.wmo.int/doc_num.php?explnum_id=3073, 2016.

Zarzycki, C. and Bond, T. C.: How much can the vertical distribution of black carbon affect its global direct radiative forcing?, Geophysical Research Letters - GEOPHYS RES LETT. 37. 10.1029/2010GL044555, 2010.

Table and figures

Table 1: Filter loading mass concentration (M_{eBC}) of the black carbon particles and filter areal loading density (deposited mass per spot area) ρ^*_i. M_{eBC} were determined by dividing the average σ_{abs} of the STAP with an assumed *MAC* of 6.6 $m^2 g^{-1}$ or based on the MAAP measurements. Usage of same filter is indicated by a separation with thick horizontal lines. Bold written entries were used for the investigation of the *rh* effect.

~~Experiment~~filter number	M_{eBC} [µg m^{-3}]	$\rho^*_{eBC,i}$ [mg m^{-2}]	
		STAP	**MA200**
#1	**44.5 (STAP)**	**14.0**	**5.4**
	43.4 (STAP)	37.9	14.4
	27.6 (STAP)	**42.9**	**16.3**
#2	**52.6 (MAAP, 2 scans)**	**2.8**	**1.1**
#3	-	**13.7 (integral of STAP)**	no data

Table 2: Average volume and mass concentration ($V_{(NH4)2SO4}$, $M_{(NH4)2SO4}$) of the loading $(NH_4)_2SO_4$ aerosol derived from the used MPSS (number of used scans in brackets) and loading areal density $\rho^*_{(NH4)2SO4}$ of the filters are given. Usage of same filter is indicated by a separation with thick horizontal lines, which means that the filter loading mass was adding up during the experiments.

~~Experiment~~filter number	$V_{(NH4)2SO4}$ [μm^3 cm^{-3}] (# scans)	$M_{(NH4)2SO4}$ [µg m^{-3}]	$\rho^*_{(NH4)2SO4}$ [mg m^{-2}]	
			STAP	**MA200**
#1	15.4 (2)	27.2	3.1	1.2
	18.6 (1)	32.9	10.5	4.0
	20.6 (3)	36.4	31.3	11.9
#2	20.6 (4)	36.5	40.8	15.5
~~#3~~	33.1 (3)	58.6	32.5	12.4
	33.5 (5)	59.3	98.7	37.6
~~#3~~	20.3 (3)	36.0	21.1	8.0
~~#4~~#4	20.3 (3)	36.0	41.9	15.9
~~#5~~	23.9 (3)	42.4	28.9	no data
~~#6~~	28.4 (4)	50.2	69.8	no data
~~#7~~#5	29.8 (2)	52.8	99.6	no data

Appendixtable 1: Coefficients of the linear regression of the instrument response to *rh* changes (*a* is slope, *b* is y-intersect, and R^2 the correlation coefficient) for the clean, ammonium sulfate and BC case for different loading areal densities ρ^*_i. The number of data-points is represented by *n*. Bold written entries represent cases with a R^2 larger than 0.8. σ indicates the standard deviation of the fitting parameters. For ammonium sulfate τ not considered.

loading aerosol	device	ρ^*_i [mg m^{-2}]	τ	*n*	*a* [Mm^{-1} %$^{-1}$]	$\sigma(a)$ [Mm^{-1} %$^{-1}$]	*b* [Mm^{-1}]	$\sigma(b)$ [Mm^{-1}]	R^2
clean	**MA200 (625 nm)**	**-**	**-**	**147**	**-0.41**	**0.00**	**-0.28**	**0.10**	**0.99**
	STAP (624 nm)	-	-	241	0.14	0.00	0.44	0.12	0.79
BC	**MA200 (625 nm)**	**1.1**	**0.98**	**18**	**-0.42**	**0.02**	**0.11**	**0.18**	**0.97**
		5.3	**0.95**	**9**	**-0.40**	**0.03**	**0.38**	**0.24**	**0.96**
		16.3	**0.82**	**9**	**-0.37**	**0.03**	**0.54**	**0.24**	**0.95**
	MA200 (625 nm, all)	-	-	**36**	**-0.41**	**0.01**	**0.28**	**0.12**	**0.96**
	STAP (624 nm)	2.8	0.93	13	0.17	0.05	0.14	0.52	0.47
		13.7	**0.78**	**33**	**0.29**	**0.01**	**1.26**	**0.37**	**0.94**
		14.0	0.74	10	0.38	0.19	0.89	1.49	0.25
		42.9	0.52	10	0.62	0.32	1.64	2.54	0.23
	STAP (624 nm, all)	-	-	66	0.29	0.02	1.00	0.48	0.72
$(NH_4)_2SO_4$	**MA200 (625 nm)**	**1.1**	**-**	**9**	**-0.38**	**0.04**	**0.39**	**0.31**	**0.93**
		4.0	**-**	**10**	**-0.42**	**0.04**	**0.00**	**0.27**	**0.94**
		8.0	**-**	**41**	**-0.41**	**0.01**	**0.10**	**0.13**	**0.97**
		11.9	**-**	**10**	**-0.40**	**0.03**	**-0.21**	**0.24**	**0.95**
		12.4	**-**	**15**	**-0.39**	**0.01**	**0.25**	**0.16**	**0.99**
		15.5	**-**	**9**	**-0.37**	**0.03**	**0.47**	**0.23**	**0.95**
		15.9	**-**	**18**	**-0.42**	**0.02**	**0.07**	**0.20**	**0.98**
		37.6	**-**	**15**	**-0.36**	**0.02**	**0.04**	**0.21**	**0.97**
	MA200 (625 nm, all)	-	-	**127**	**-0.40**	**0.01**	**0.10**	**0.07**	**0.97**
	STAP (624 nm)	3.1	-	10	0.17	0.09	0.35	0.72	0.23
		10.5	-	10	0.19	0.09	0.33	0.72	0.28
		21.1	-	34	0.20	0.04	0.73	0.49	0.42
		28.9	**-**	**90**	**0.23**	**0.01**	**0.92**	**0.34**	**0.81**
		31.3	-	10	0.19	0.09	0.34	0.71	0.28
		32.5	**-**	**13**	**0.19**	**0.02**	**0.35**	**0.36**	**0.82**
		40.8	-	10	0.21	0.10	0.42	0.79	0.28
		41.9	-	16	0.20	0.05	0.16	0.64	0.47
		69.8	**-**	**56**	**0.19**	**0.01**	**0.89**	**0.16**	**0.96**
		98.7	**-**	**14**	**0.24**	**0.03**	**0.28**	**0.39**	**0.86**
		99.6	**-**	**33**	**0.19**	**0.01**	**0.87**	**0.24**	**0.95**
	STAP (624 nm, all)	**-**	**-**	**296**	**0.21**	**0.01**	**0.71**	**0.14**	**0.82**

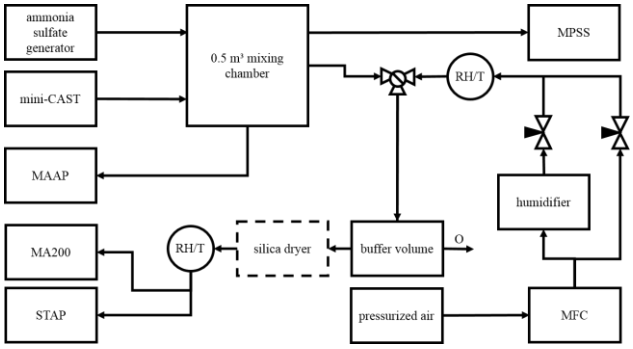

Figure 11: Scheme of the experimental setup. The volumetric flow rates of two air-streams were controlled with two needle valves to produce humidified particle free air via mixing of wet and dry particle free air. It was ensured that the sum of both flow s was larger than the volumetric flow of both absorption photometer investigated here. Any exceeding airflow was directed to a buffer volume with an overflow outlet (O). The relative humidity and the temperature of the air were recorded directly after the hum idifier and shortly before the photometers with the *rh* and *T* sensors.

710

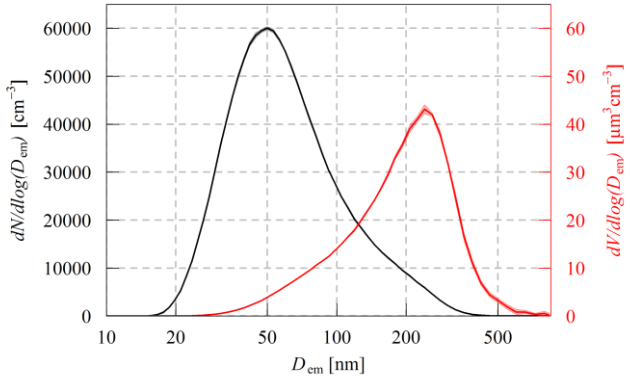

Figure 22: Average particle number (black) and volume size distributions (red) of the ammonium sulfate aerosol loaded on the filters in the MA200 and STAP during experiment #2 of the ammonium sulfate loading experiments. The average volume of 20.6 µm³ cm⁻³ is calculated from four scans. The shaded area indicate the standard deviation of the mean. D_{em} refers herein to the electrical mobility diameter of the aerosol particles.

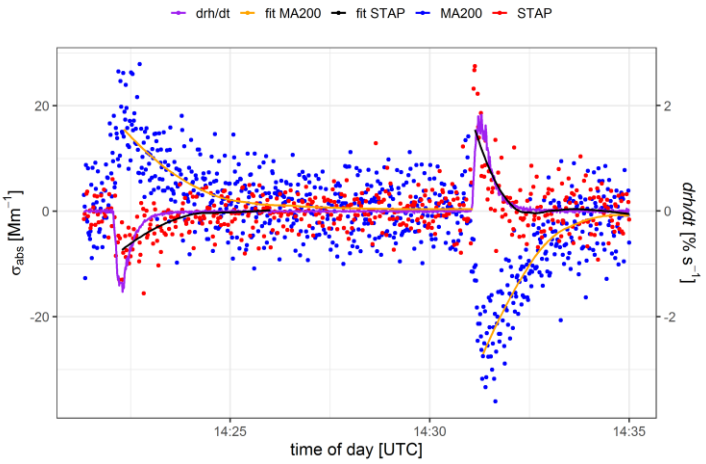

Figure 3: 1 Hz raw data of σ_{abs} at 625 nm measured by the MA200 (blue points) and recalculated at 624 nmSTAP200 (red points), the smooth fit through the measurements (orange and black), and d*rh*/d*t* (purple line).

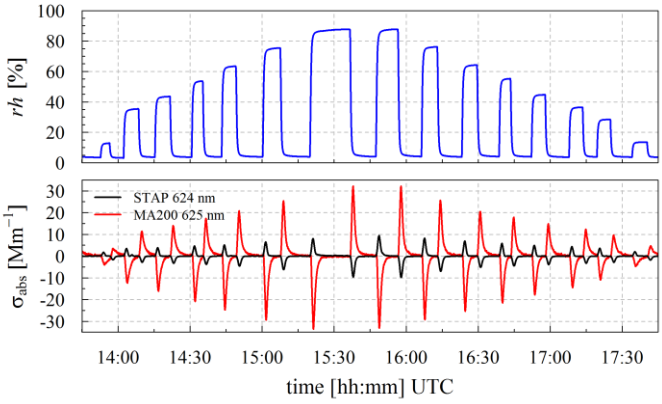

Figure 4: Time series of *rh* (top panel) and absorption coefficient (bottom panel) measured with STAP (624 nm; black) and MA200 (625 nm; red) with clean filters.

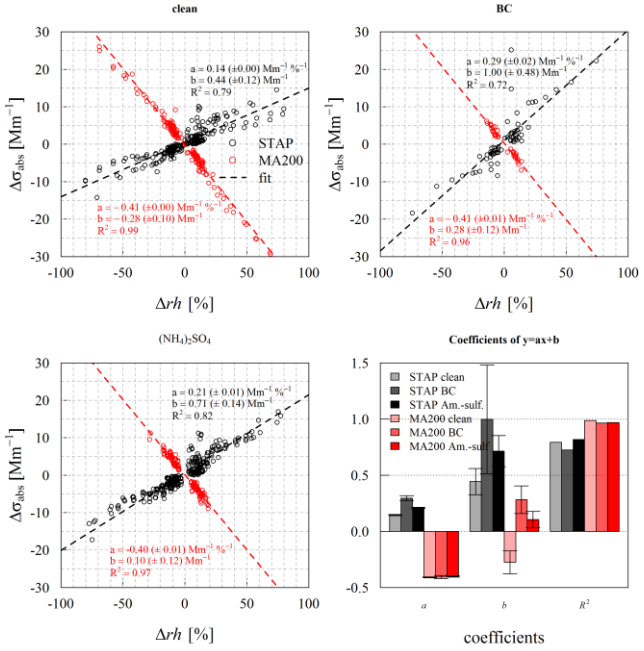

Figure 5: Scatter plot (dots) of all observations of the absolute excursion of σ_{abs} ($\Delta\sigma_{abs}$) in dependence of the absolute change in *rh* (Δrh), its linear regression fit as well as the summarizing boxplot of the linear regression fit are shown for the three investigated states (clean, loaded with BC and ammonium sulfate) at 624 nm (STAP, black colors) and 625 nm (MA200, red colors). Descriptive coefficients are given in Appendixtable 1~~Appendixtable 1~~.

Formatiert: Schriftfarbe: Automatisch

720

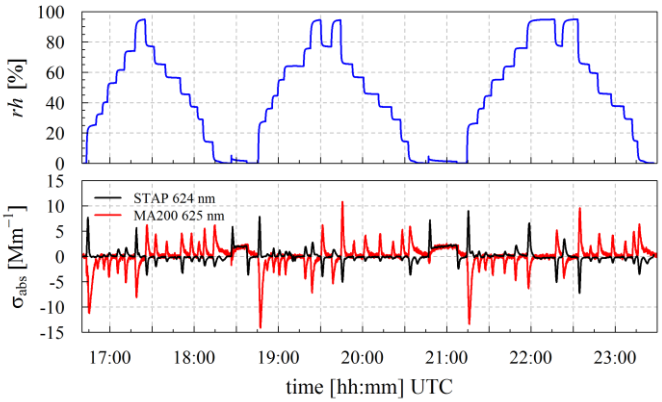

Figure 6: *rh* of the air stream sampled by the MA200 and the STAP (upper panel) and σ_{abs} measured by MA200 and STAP at 625 (624) nm (lower panel). First up and down ramp of *rh* conducted with clean filter, second and third under conditions with filter loaded with ammonium sulfate. Loading periods around 18:30 and 21:00 UTC.

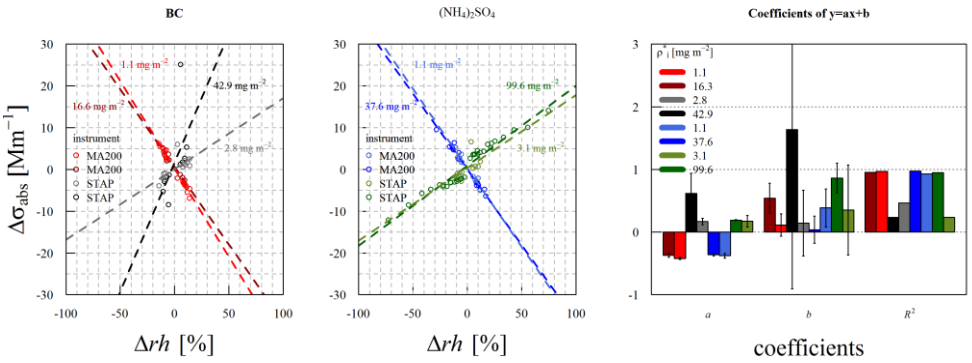

Figure 7: Scatter plot of change in absorption ($\Delta\sigma_{abs}$) in dependence of the absolute change in *rh* (Δrh) separated into the different loading states (loaded with BC and ammonium sulfate) and minimum and maximum loading areal density on the filter. Dashed and colored lines represent the linear regression fit. Red and blue colors indicate MA200 at 625 nm and black and green colors indicate STAP at 624 nm. In the first panel BC loading is shown whereas in the second panel the ammonium sulfate case is displayed. Coefficients of the linear regression fit are displayed in panel 3. Shading of color in the linear fits and of the points are same as in panel 3.

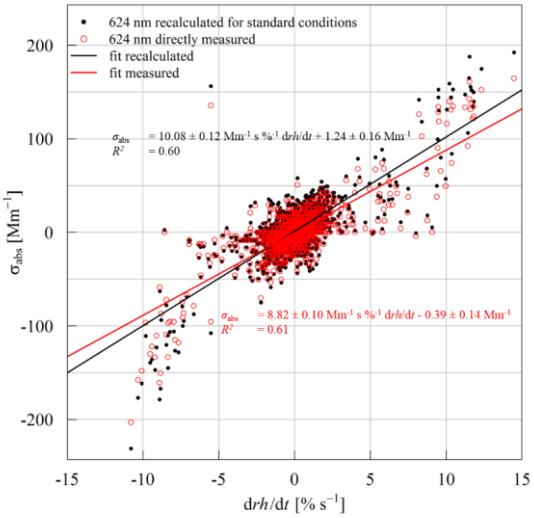

Figure 8: Scatterplot of σ_{abs} and change rate of *rh* (d*rh*/d*t*) at 624 nm derived directly from STAP without any corrections (red) and recalculated σ_{abs} at 624 nm including corrections to standard conditions (black). Linear fit equations and correlation coefficient are given in the corresponding colors.

725

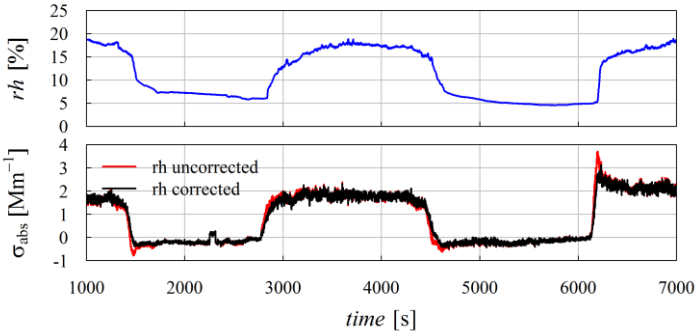

Figure 9: Time series of *rh* before the inlet of the STAP (blue, upper panel) and recalculated σ_{abs} (~~floating~~ running 60 s mean of 1 Hz calculations) at standard conditions corrected (black) and uncorrected (red) for *rh* changes.

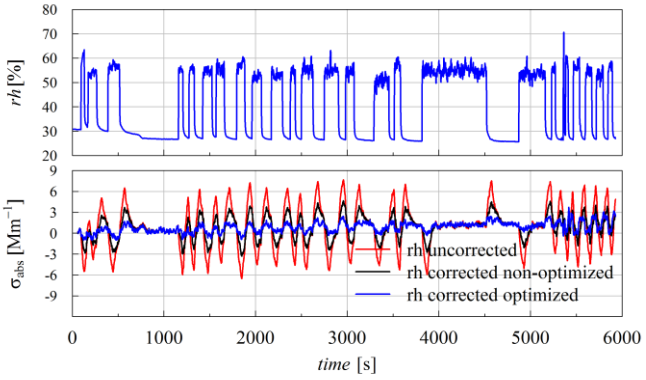

Figure 10: Time series of a laboratory measurement of σ_{abs} conducted with the MA200 without a filter. Upper panel shows the *rh* of the aerosol sample and the lower panel displays the 60 s ~~floating~~ running average of measured σ_{abs} at 1 Hz time resolution and 625 nm uncorrected and biased by *rh* changes (red) and corrected with the modelled σ_{abs} derived with the ARMA-X model (black).